Industrial & Engineering Chemistry Research
pubs.acs.org/IECR
Article

Multicomponent Refrigerant Separation Using Extractive Distillation with Ionic Liquids

Ethan A. Finberg, Tessie L. May, and Mark B. Shiflett*

Cite This: https://doi.org/10.1021/acs.iecr.2c00937 Read Online

ACCESS | Metrics & More | Article Recommendations | Supporting Information

ABSTRACT: Hydrofluorocarbon refrigerants are being phased out over the next two decades due to concerns about high global warming potential. In order to separate refrigerant mixtures that form azeotropes, new technologies will be required. Currently, fractional distillation is unable to efficiently separate azeotropic refrigerant mixtures. Extractive distillation using an ionic liquid as the entrainer offers a solution. Vapor−liquid equilibria data for refrigerants difluoromethane (HFC-32), pentafluoroethane (HFC-125), 1,1,1,2-tetrafluoroethane (HFC-134a), 1,1,1-trifluoroethane (HFC-143a), chlorodifluoromethane (HCFC-22), propane (HC-290), and isobutane (HC-600a) and ionic liquid 1-butyl-3-methylimidazolium hexafluorophosphate ([C_4C_1im]- [PF_6]) was regressed using the Peng−Robinson equation of state with

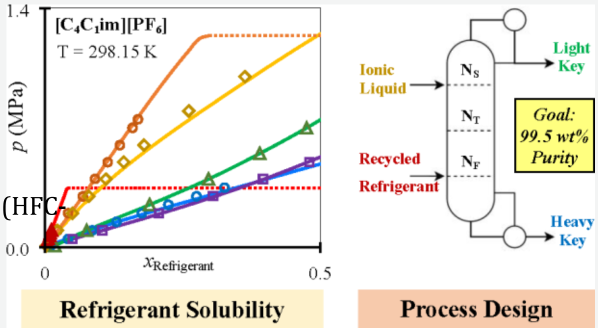

the van der Waals 1-parameter mixing rule and Boston−Mathias nonideal correction. Process flow diagrams using ASPEN
simulations were prepared for demonstrating how multicomponent mixtures of these refrigerants can be separated. Opportunities for measuring and modeling the solubility of new refrigerants in ionic liquids are discussed, and

1. INTRODUCTION

Hydrofluorocarbons (HFCs) and HFC mixtures have been used globally as refrigerants since the 1990s because of the restrictions on chlorofluorocarbons (CFCs) and hydrochloro- fluorocarbons (HCFCs). Chlorinated fluorocarbons are linked to the depletion of the Earth's ozone layer[1] and were banned due to high ozone depletion potential (ODP)[2] according to the Montreal Protocol in 1987. Global warming potential (GWP) was introduced by Houghton et al. in 1990 to determine the effect on the greenhouse gas theory.[3] Even though HFCs have a zero ODP, some HFCs have a high GWP ranging from 1000 up to 5000[4] on a 100 year basis (where CO_2 = 1.0). In 2019, fluorinated gases were estimated to account for three percent of total greenhouse gas emissions based on equivalent metric tons of CO_2.[5]

The increasing concern of the high GWP for certain HFCs has led to the introduction of international policies such as the 1997 Kyoto Protocol to the UNFCCC,[6] the 2015 European Fluorinated Greenhouse Gas (EU F-Gas) Regulations,[7] the 2016 Kigali Amendment (the sixth amendment to the Montreal Protocol),[8,9] and the 2020 American Innovation and Manufacturing (AIM) Act.[10] These policies propose reducing the production of HFCs by more than 80% within the next two decades. Moreover, the Montreal Protocol calls for a phaseout of HCFCs in all developed countries by 2020 and in all developing countries by 2040.

The refrigerant industry is currently transitioning to the next-generation refrigerants, hydrofluoroolefins (HFOs) and HFO/HFC refrigerant blends, to replace HFCs in many applications;[11] however, there are no pure HFCs that satisfies the criteria for minimizing GWP, ODP, and flammability.[12] Alternatives such as HFOs and HFO blends with HFCs, hydrocarbons (HCs), and inorganic compounds such as CO_2 are being proposed as replacements for air-conditioning and refrigeration applications.

Disposal of HFCs at "end-of-life" has become an issue, and many are illegally vented to the atmosphere. The alternative is incineration, which is energy-intensive and produces toxic wastes such as sodium and calcium fluorides that have to be landfilled. A more environmentally friendly alternative would be to separate high-GWP refrigerants from low-GWP refrigerants, such as difluoromethane (HFC-32, GWP = 670), for use in future HFO/HFC blends. The high-GWP refrigerants can be used as fluorinated feedstocks for producing new products with low-GWP such as future HFOs[13] and fluoropolymers. Research using HFCs as reactants is a field ready for further investigation.

Received: March 23, 2022
Revised: June 6, 2022
Accepted: June 14, 2022

ACS Publications

https://doi.org/10.1021/acs.iecr.2c00937
Ind. Eng. Chem. Res. XXXX, XXX, XXX−XXX

Developing a separation process to purify HFCs from refrigerant mixtures can be challenging since many of these mixtures are azeotropic or near azeotropic, making separation difficult to impossible using conventional distillation methods. Only advanced separation processes provide an alternative for recovering refrigerant blends, such as absorption in liquid entrainers,[14,15] adsorption on materials such as zeolites,[16] and membrane separation technologies.[17] Project EARTH (Envi- ronmentally Applied Research Towards Hydrofluorocarbons) is developing environmentally responsible materials and technology to separate azeotropic HFC mixtures and recycle the pure component refrigerants. This work focuses on modeling extractive distillation for the separation of azeotropic refrigerant mixtures using ionic liquids (ILs).

Extractive distillation[18] is a form of distillation commonly used for the separation of homogeneous azeotropic mixtures or close-boiling solvents.[19] Commercial examples include olefin/ paraffin (alkene/alkane), aliphatic/aromatic hydrocarbons, aromatic/aromatic hydrocarbons, and dehydration separa- tions.[20]

The goal of this paper is to show that multicomponent refrigerant mixtures that contain azeotropic compositions can be separated using unit operations such as extractive distillation with ionic liquid entrainers. Currently, these mixtures cannot be separated using conventional distillation and are stockpiled, illegally vented, or incinerated. An environmentally responsible alternative is to separate the refrigerant mixtures into pure components that can be recycled and repurposed to reduce the amount of new HFCs manufactured, ultimately decreasing overall global warming.

This work provides a design for the separation of multicomponent azeotropic refrigerant mixtures using flash separation, conventional distillation, and extractive distillation. Seven common refrigerants, including HFC-32 (difluoro- methane), HFC-125 (pentafluoroethane), HFC-134a (1,1,1,2-tetrafluoroethane), HFC-143a (1,1,1-trifluoroethane), HCFC-22 (chlorodifluoromethane), HC-290 (propane), and HC-600a (isobutane), have been included in this study. Global market trends were used to estimate probable multicomponent mixture compositions for reclaimed refrigerant gases. Binary interaction parameters have been regressed to predict the global phase behavior, vapor−liquid equilibrium (VLE), and liquid−liquid equilibrium (LLE) over the entire refrigerant + IL composition range. The quality of experimental data based on model regressions is discussed, and this work also organizes an extensive literature review for extractive distillation with ILs, refrigerant solubility in ILs, and binary equilibrium data of refrigerants.

1.1. Global Refrigeration.

The Clean Energy Manufacturing Analysis Center (CEMAC) estimates the global production of refrigerants annually. The current estimate of almost 800 kiloton (kt) can be divided into two categories: heating, ventilation, and air conditioning (HVAC) systems (399 kt) and refrigeration equipment (387 kt).[11] The refrigerant distribution for these totals is provided in Table S1 in the Supporting Information (SI).

HFC-32, HFC-125, HFC-134a, and HFC-143a are the largest-volume HFC refrigerants produced annually, while R-404A, R-407C, and R-410A are the largest-volume refrigerant mixtures produced. HCFC-22 is still in use and remains in circulation, even though HCFC-22 is no longer sold as a refrigerant.

The annual kt of refrigerant for HVAC and refrigeration applications was used to estimate compositions for hypo- thetical mixtures of reclaimed gases shown in Table 1. The

Table 1. Weight Fraction Distribution of Refrigerants[11]

	refrigeration		HVAC	
components	(kt)	(wt %)	(kt)	(wt %)
HFC-32	11	2.8	104.5	26.2
HFC-125	46.2	11.9	94.8	23.7
HFC-134a	34.2	8.8	37.8	9.5
HFC-143a	41.6	10.7		
HCFC-22	203	52.5	159.0	39.8
other	51	13.2	3	0.8
total	387	100	399	100

"other" refrigerants used in HVAC and refrigeration applications, not shown in Table 1, are primarily HFO- 1234yf (2,3,3,3-tetrafluoropropene), HCFC-142b (1-chloro- 1,1-difluoroethane), HFC-152a (1,1-difluoroethane, or DFE), HC-290 (propane), HC-600a (isobutane), R-717 (ammonia), and R-744 (CO_2).

The two largest-volume hydrocarbons used primarily for refrigeration applications are HC-290 and HC-600a. For refrigeration applications, the "other" refrigerant composition is assumed to be an even split between HC-290 and HC-600a. Refrigerant HC-600a is not typically used in HVAC systems, so the "other" represented in the HVAC composition is assumed to be only HC-290. The focus of this paper is to develop a separation process for HFCs, HCFCs, and HCs, so inorganic refrigerants R-717 and R-744, as well as HFO-1234yf, were excluded. Also, compositions of HCFC-142b and HFC-152a were assumed to be negligible, since the use of these refrigerants in HVAC and refrigeration applications is small. The simulations in this work were based on compositions shown in Table 1.

1.2. Extractive Distillation with Ionic Liquids.

Extractive distillation uses an entrainer to absorb (i.e., entrain) a component, breaking the azeotrope, or to modify the volatilities for close-boiling nonazeotropic VLE regions, and result in more efficient separation. The entrainer and the entrained component leave the bottoms of the extractive distillation column and are fed into another unit operation (usually a flash column or second stripping column) to purify the solute and recover the entrainer. Entrainers are typically low-volatility, high-boiling solvents that make recovery simple and efficient.

There are four criteria for selecting an entrainer: (i) high miscibility with the feed to avoid two-liquid phases in the distillation process, (ii) absorption selectivity of the feed components, (iii) low volatility to ensure an easy solvent recovery, and (iv) nonazeotropic with the feed components. Five types of entrainers have been described for extractive distillation: liquid solvents, solid salts (or dissolved salts), a mixture of liquid solvents and solid salts, hyperbranched polymers, and ionic liquids (ILs).[21] Organic liquid solvents have been the primary choice for entrainers, but ILs have shown higher selectivity for some processes.[22,23]

Ionic liquids are typically composed of a large organic cation and an inorganic anion, allowing these materials to exist in a liquid state at (or near) room temperature, unlike most salts.[24] The names and abbreviations of cations and anions represented in this work are shown in Table S2.

https://doi.org/10.1021/acs.iecr.2c00937

Table 2. Published Data on the Solubility of Refrigerants in Ionic Liquids

	$[C_2C_1im][Ac]$	$[C_2C_1im][BF_4]$	$[C_2C_1im][BEI]$	$[C_2C_1im][Cl]$	$[C_2C_1im][OTf]$	$[C_2C_1im][PFP]$	$[C_2C_1py][PFBS]$	$[C_2C_1im][Tf_2N]$	$[C_2C_1im][TFES]$	$[C_2C_1im][SCN]$	$[C_2C_1py][PFBS]$	$[C_3C_1im][Cl]$	$[C_4C_1im][Ac]$	$[C_4C_1im][BF_4]$	$[C_4C_1im][HFPS]$	$[C_4C_1im][PF_6]$	$[C_4C_1im][Tf_2N]$	$[C_4C_1im][TPES]$	$[C_4C_1im][TTES]$	$[C_4C_1im][SCN]$	$[C_6C_1im][BF_4]$	$[C_6C_1im][Br]$	$[C_6C_1im][Cl]$	$[C_6C_1im][FAP]$	$[C_6C_1im][I]$	$[C_6C_1im][PF_6]$	$[C_6C_1im][Tf_2N]$	$[P_{(14)666}][Cl]$	$[P_{(14)666}][TMPP]$
HFC-32	73	74	75, 76	77	73, 74, 78	73	73	75, 76 73	75	79	73	77	14, 75	14, 76, 80	75	76, 80 14		75	75	14, 75		77	14, 77	14	77		81	77	82
HFC-125	73			77	73	73	73	73, 83		84	73	77	14	14		14, 76 80, 85				14		77	14, 77	14	77		81	77	86
HFC-134a	73	74	76, 87		73, 74	73	73	73, 88-91		79	73				76, 87	76, 80, 92		76, 87	76, 87		88					88	88, 93		86
HFC-143a																80, 92											94		86
HCFC-22								95	95					95		76, 95													
HFO-1234yf	96	97			74			74		79			96	98		99	98				97, 100					99, 100	101	96	
HC-290								102									103										104	105	106
HC-600a								107						108		108	107, 108										107, 109	105	109

Many ILs have high thermal and chemical stability with a wide liquid range making them an excellent choice for entrainers. Ionic liquids also have extremely low vapor pressure (e.g., $<1 \times 10^{-5}$ Pa) and low volatility, which significantly reduces the amount of the entrainer that can contaminate the distillate (one of the trade-offs in using extractive distillation).
Ionic liquid properties, such as density, viscosity, gas solubility, and selectivity can also be designed to maximize separation efficiency by selecting the appropriate cation and anion. For example, by designing an IL with low viscosity, the mass transfer efficiency can be increased, and the overall efficiency of the separation process may be improved.[25] Extensive studies
and reviews on gas solubility in ILs[26−28] have been published,
but only a few works describe the separation of azeotropic mixtures using ILs as entrainers.[29]

Ionic liquids were first introduced as entrainers in 2001 by
the BASF Chemical Company and patented in 2004 by Wolfgang Arlt et al.[30,31] Only two institutions, BASF[32] and Eindhoven University of Technology (EUT),[33] have published details regarding the experimental setup for testing extractive distillation with ILs. However, 33 articles have been published on the simulation of ILs as entrainers for extractive
distillation.[34−66] Table S3 provides a summary of all of the
published material on extractive distillation with IL entrainers, including the (i) components being separated, (ii) IL entrainer, and (iii) thermodynamic model used to predict the equilibrium of the system. Most of these separations were binary systems; however, the italicized labels shown in Table S3 represent multicomponent mixtures.

Thermodynamic models are correlated by either activity coefficient models using the γ−φ method or equations of state (EoS) using the φ−φ method. In some cases, group contribution methods, such as the UNIFAC-Lei,[67] UNIFAC- IL,[68] and COSMO-SAC[69] models, were used to predict the activity coefficient thermodynamic models. In other cases,
experimental data was fitted using either an activity coefficient model, such as NRTL,[70] or EoS, such as the Cubic Plus Association (CPA),[71] soft-SAFT,[72] or Peng−Robinson. Group contribution methods can also be used to screen hundreds of ILs and find candidates for separation; then, experimental data can be measured and fitted to an activity coefficient model or EoS.

https://doi.org/10.1021/acs.iecr.2c00937

Systems that used activity coefficient models and did not define an EoS for the vapor phase assumed that the vapor phase was ideal ($\varphi^V = 1$). For polar compounds such as HFCs, the ideal gas mixture in the vapor phase is not a good assumption, and an EoS such as that described in Table S3 for the CO_2/tetrafluoroethylene (TFE)[63] system is necessary for making accurate vapor-phase calculations. Moreover, if one of the components is at or near the critical point, such as HFC solubility in ILs occurring at high temperatures or pressures, an EoS for modeling the vapor phase should be considered.

1.3. Refrigerant Solubility in Ionic Liquids.

The solubility of refrigerants in ILs can be measured using a variety of techniques including chromatography, ebulliometry, gravimetric, and volumetric methods. A literature review for the solubility (i.e., VLE data) of HFC-32, HFC-125, HFC-134a, HFC-143a, HCFC-22, HFO-1234yf, HC-290, and HC-600a in ILs was conducted. A detailed list containing 38 references is provided in Table 2.[14,73−109]

Literature works containing only the dilute regime, or Henry's Law constants, were not included in Table 2 but include the following three sources: (i) HFC-143a in $[C_6C_1im][Tf_2N]$, $[C_6C_1im][OTf]$, and $[C_6C_1im][BF_4]$;[110] (ii) HC-290 and HC-600a in $[C_4C_1im][BF_4]$, $[C_4C_1im][PF_6]$, $[C_2C_1im][OTf]$, and $[C_2C_1im][Tf_2N]$;[111] and (iii) HC-290 in $[C_2C_1im][BF_4]$, $[C_6C_1im][BF_4]$, and $[C_4C_1im][Tf_2N]$.[112] The binary system HFC-143a/$[C_2C_1im][Tf_2N]$ was also removed from Table 2 since the article only included NRTL parameters for LLE data and no VLE solubility data.[83]

Asensio-Delgado et al. prepared a similar literature review for fluorinated refrigerant gases in ILs but did not include hydrocarbon refrigerants, such as HC-290 and HC-600a.[65] The ILThermo NIST database was also a useful resource for obtaining IL physical property data.[113]

In general, published solubility data was available for the majority of these eight refrigerants in the ILs $[C_2C_1im][Tf_2N]$, $[C_4C_1im][PF_6]$, and $[C_6C_1im][Tf_2N]$. There are many opportunities for future work to measure and model the solubility of refrigerants in ILs, hence the blank spaces in Table 2. Moreover, there is no known solubility data for HCFC-142b in ILs. In this work, the IL $[C_4C_1im][PF_6]$ was selected for simulations because of the VLE data available for seven of the

https://doi.org/10.1021/acs.iecr.2c00937

refrigerants and the higher selectivity than using [C_2C_1im]- [Tf_2N], as discussed in our previous work.[66]

2. REGRESSION

2.1. Thermodynamic Model: Peng−Robinson. The Peng−Robinson equation of state (PR-EoS),[114] shown in eq 1, was used to calculate phase behavior by fitting VLE experimental data for the binary systems of HFC-32, HFC-125, HFC-134a, HFC-143a, HCFC-22, HC-290, and HC-600a, as well as solubility in [C_4C_1im][PF_6].

$$P = \frac{RT}{V - b} - \frac{a}{V(V + b) + b(V - b)} \tag{1}$$

The PR-EoS parameters a and b are a function of the pure component critical properties: critical temperature (T_c), critical pressure, (P_c), and the acentric factor (Ω). These properties as well as the physical properties (T_b and MW), volume and compressibility critical properties (V_c and Z_c), and ideal gas heat capacities ($\Delta C_{P,IG}$) are required to regress the VLE data using the PR-EoS in the ASPEN software. The critical properties for ILs are considered pseudoproperties since the T_c is above the IL decomposition temperature. The critical properties, including Ω and T_b, for [C_4C_1im][PF_6] were calculated using a group contribution method proposed by Valderrama and Robles,[115,116] and $\Delta C_{P,IG}$, for [C_4C_1im]-[PF_6] was estimated as a function of T using the Joback method published by Ge et al.[117] The pseudocritical properties and $\Delta C_{P,IG}$ are provided in the SI in Table S4 and Figure S1. The van der Waals 1-parameter (vdW1) mixing rule was selected to define the PR-EoS mixing parameters a and b as shown in eqs 2 and 3.

$$a_m = \sum_{i=1}^{C}\sum_{j=1}^{C} x_i x_j (1 - k_{ij})(a_i a_j)^{0.5} \tag{2}$$

$$b_m = \sum_{j}^{C} x_i b_i \tag{3}$$

Mixing rules are defined by the pure component parameters for each species i and j and the vapor or liquid composition of each component, x_i. Experimental VLE data was fitted to the PR-EoS with the vdW1 mixing rule using the temperature- dependent binary interaction parameter, k_{ij}, shown in eq 4.

$$k_{ij} = k_{ij}^{(1)} + k_{ij}^{(2)} T + \frac{k_{ij}^{(3)}}{T} \tag{4}$$

The interaction parameter is assumed to be symmetric (k_{ij} = k_{ji}), and only the linear temperature-dependent parameter, $k_{ij}^{(2)}$, is regressed

The B−M method is used for multicomponent mixtures and was recommended for the Peng−Robinson EoS when modeling polar, nonideal chemical systems with asymmetric mixing rules. Unlike the vdW parameter k_{ij}, the B−M correction parameter l_{ij} can be regressed asymmetrically with $l_{ij} \neq l_{ji}$. Parameter l_{ij} carries the same temperature-dependencies as parameter k_{ij} (shown in eq 4) and is assumed to be symmetric (l_{ij} = l_{ji}) in this work. Only the linear temperature- dependent parameter, $l_{ij}^{(2)}$, is regressed in this work.

2.2. Maximum Likelihood. The maximum likelihood (ML) technique[119] was selected for regressing experimental data. The ML method has a minimizing-objective function, weighed by the error of each experimental coordinate, and fits the experimental data point (exp) to the model's regression data point (reg). Each data point represents four experimental coordinates: temperature (T), pressure (P), liquid composition of component i (x_i), and vapor composition of component i (y_i). When incorporating the four experimental coordinates, T, P, x_i, and y_i, the ML objective function can be written as shown in eq 7.

$$\min Q = \sum_{d=1}^{D} w_d \sum_{n=1}^{N} \left[\left(\frac{T^{exp} - T^{reg}}{\sigma_T}\right)_n^2 + \left(\frac{P^{exp} - P^{reg}}{\sigma_P}\right)_n^2 + \left(\frac{x_i^{exp} - x_i^{reg}}{\sigma_x}\right)_n^2 + \left(\frac{y_i^{exp} - y_i^{reg}}{\sigma_y}\right)_n^2 \right] \tag{7}$$

The errors (σ) were assumed to be similar for all data sets with the following values: σ_T = 0.1 K, σ_P = 0.1% MPa, σ_x = 0.1 mol %, σ_y = 1.0 mol %. The vapor composition error was assumed to be an order of magnitude larger than the liquid composition. If multiple data sets (D) are used in the regression, an additional weighting factor can be included for one data set (d) by scaling the objective function with a multiplier (w_d). In this work, none of the refrigerant binary mixtures with multiple data sets were weighed (w_d = 1).

Error estimations were calculated to determine the quality of results on each experimental variable (T, P, x_i, y_i). Error estimations can be categorized into two methods: deviation (i.e., error) and relative deviation (i.e., error percent). Table S5 provides examples of error estimations.

Relative deviation error analyses, such as RMSE% and AARD%, are acceptable methods for ratio data, such as mass, absolute pressure, or temperature in Kelvin, where a measurement of zero represents the absence of a value. However, relative deviation is not an adequate method for interval values such as gauge pressures, temperatures in Celsius in this work.

or Fahrenheit, and compositions (x_i and y_i), where the measurement is represented by an interval

For highly nonideal systems, such as IL solubility, the Boston−Mathias (B−M)[118] correction was added to the vdW1. This method provides a second binary interaction parameter for regression, l_{ij}, as shown in eqs 5 and 6, where a_0 represents the vdW1 mixing rule from eq 2, and a_1 represents the B−M correction.

$$a_m = a_0 + a_1 \quad (5)$$

$$a_1 = \sum_{i=1}^{c} x_i \sum_{j=1}^{c} x_j [(l_{ij})((a_i a_j)^{0.5})^{3}] \quad (6)$$

from a reference zero value. Calculating the relative deviation of an interval value produces inconsistent and very large error estimations as the experimental value approaches zero. Since the error in composition (x_i and y_i) cannot be analyzed using relative deviation, the average absolute deviation (AAD) was calculated for each of the four experimental variables. The AAD can be calculated to include multiple data sets for one binary system; however, since one data set might be inconsistent and less accurate, each data set was analyzed individually.

2.3. Refrigerant Binary Regression. Mixing parameters $k_{ij}^{(1)}$ and $k_{ij}^{(2)}$ from the vdW1 mixing rule were defined by regressing VLE data for binary mixtures composed of seven refrigerants: HCFC-22, HFC-32, HFC-134a, HFC-125, HFC-

Table 3. Binary Refrigerant Regression Summary

(i)	(j)	N_{points}	N_{temp}	temperature range (K)	$k_{ij}^{(1)}$ ($\times10^1$)	$k_{ij}^{(2)}$ ($\times10^4$)	AAD x_j (%)	ref
HCFC-22	HFC-32[a]	13	1	283.15	0.072		0.15	122
	HFC-125[d]				1.955	−7.810		
	HFC-134a	20	3	273.16−323.16			0.25	123
		60	5	343.81−372.12	−0.132	0.867	0.14	124
	HFC-143a[a]	11[c]	1	275	−0.092		0.00	125
	HC-290[a]	12	1	273.15	0.847		0.32	126
	HC-600a[d]				0.486	0.933		
HFC-32	HFC-125	66	5	265.15−303.15	0.216	−0.619	0.32	127
	HFC-134a	124	11	258.15−343.15	−0.162	0.506	*1.12*	128
	HFC-143a	60	6	263.15−313.15	0.281	−0.508	0.24	129
	HC-290	101	7	253.15−323.15	1.685	0.802	0.16	130
	HC-600a	40	2	260−310			0.51	131
		32	5	301.8−321.8	1.695	0.950	*1.39*	132
HFC-125	HFC-134a	34	5	263.15−303.15			0.24	133
		49	7	303.75−363.15	−0.043	0.101	0.58	134
	HFC-143a[b]	16	3	273.15−313.15	0.187	−0.647	0.11	135
	HC-290	117	8	253.15−323.15	1.656	−0.627	0.11	130
	HC-600a	40	3	293.15−313.15	2.735	−4.237	0.31	136
HFC-134a	HFC-143a	54	6	263.15−313.15	0.331	−1.289	0.28	137
	HC-290	66	6	273.15−323.15	1.818	−0.428	0.30	138
	HC-600a	28	2	293.66−303.68			0.34	139
		32	2	303.2−323.2	2.193	−1.927	0.48	132
HFC-143a	HC-290	42	6	268.15−318.15			0.13	140
		52	6	313.15−363.15	0.656	2.008	0.28	141
	HC-600a[a]	20	2	323.15−333.15	1.620	−1.092	0.44	142

[a]The only binary data source available. [b]4 of the 16 points not regressed at 273.15 K due to inconsistencies. [c]Only liquid composition measurements. [d]Simulated data provided by Chemours.

143a, HC-290, and HC-600a. In some cases, multiple data sets were combined from various sources to expand the regression over a broader *TPxy* range. For example, two literature sources for HCFC-22/HFC-134a with VLE data from 343.81 to 371.12 K and from 273.15 to 323.15 K were combined to define more accurate temperature-dependencies in the regression.

For the case where the binary equilibrium data was measured at only one temperature, the temperature-dependent parameter, $k_{ij}^{(2)}$, was set equal to zero (e.g., HCFC-22/HFC-32 data only available at T = 283.15 K). Initially, binary data sets with multiple temperatures were regressed without the temperature-dependent parameter $k_{ij}^{(2)}$ to test if regressing $k_{ij}^{(1)}$ can accurately predict experimental VLE data over a broad temperature range. Results showed that $k_{ij}^{(2)}$ was only necessary to predict VLE for large temperature ranges (∼100 K); therefore, binary systems regressed at one temperature can accurately predict VLE at other temperatures for some systems.

Currently, there is no published VLE data for two binary systems (HCFC-22/HFC-125 and HCFC-22/HC-600a), and four binary systems only have one reference. The VLE data for HCFC-22/HFC-143a had 11 data points, but these do not include y_i measurements. Group contribution methods have been proposed to predict VLE for refrigerants,[120] but simulated data was provided and regressed to calculate the vdW mixing parameter k_{ij} with the PR-EoS.[121]

A summary for the binary VLE regression results ($k_{ij}^{(1)}$ and $k_{ij}^{(2)}$) is shown in Table 3,[122−142] where column "x_i" represents had a total of 16 data points to regress, but four of the six data points at 273.15 K were considered outliers and were excluded from the regression.

Excellent fits were obtained for most systems with an AAD in composition of <1 mol %. The binary systems HFC-32/HC-600a and HFC-32/HFC-134a had an AAD of 1.39 and 1.12 mol % with minor scatter in the composition as shown in Figures S3a and S4b; however, the overall trends were still a good fit with the experimental data.

The vapor composition (y_i) had a larger AAD, which was expected since the inputted errors for the ML objective function were weighed toward x_i rather than y_i (σ_x = 0.1 mol % and σ_y = 1.0 mol %). For all binary systems, the average AAD for x_i was 0.011%, with a maximum deviation of 0.061 mol %, and y_i showed an average of 0.734 mol % with a maximum deviation of 2.735 mol %; pressure had an average AAD of 0.002 MPa with a maximum deviation of 0.009 MPa and an average temperature of 0.4 K with a maximum deviation of 1.8 K.

Examples of the regression compared with experimental data for binary systems containing HFC-32, HFC-125, HFC-134a, and HFC-143a with HC-290 are shown in Figure 1. In some cases where multiple sources provided *Pxy* data at the same isotherm, a comparison was made between the regression and the additional literature results [e.g., HFC-32/HC-290 (Figure 1a)[143] and HFC-125/HC-290 (Figure 1b)[144,145]]. All *Pxy* diagrams showing the experimental values with the regressed equilibrium models are provided in the SI (see Figures S2−S6).

the overall AAD in composition of both x_i and y_i. The AAD for each variable (T, P, x_i, y_i) for all binary systems can be found in the SI (see Table S6). The binary system HFC-125/HFC-143a

Many of the binary systems had limited VLE data and in some cases only one source was available (see Table 3, data denoted by footnote a). This provides an opportunity for

https://doi.org/10.1021/acs.iecr.2c00937

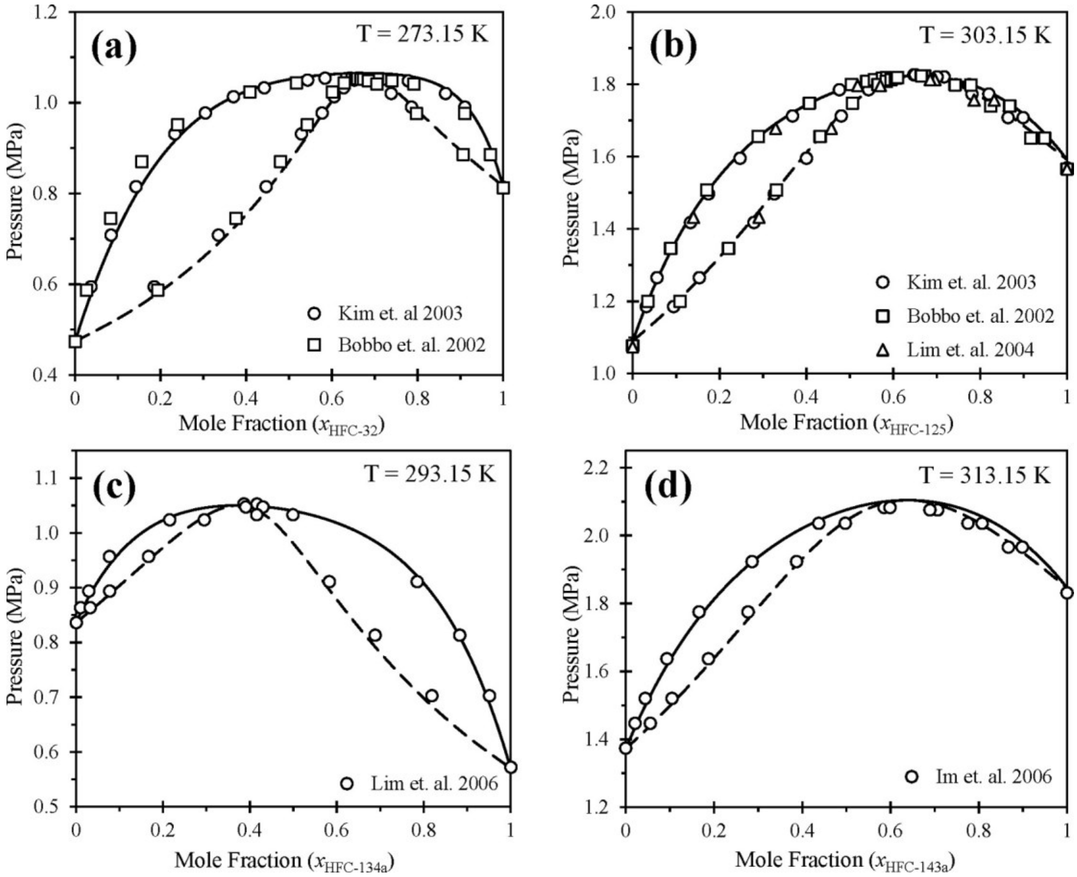

Figure 1. Regressed *TPxy* data (○) for (a) HFC-32, (b) HFC-125, (c) HFC-134a, and (d) HFC-143a in HC-290 from Table 3, with comparable isothermal data for HFC-32 (□[143]) and HFC-125 (□,[144] Δ[145]) from other sources.

future works to measure additional VLE data for these systems. Once regressions were completed, azeotropes were simulated at normalized pressures. In the case of HFC-125/HC-290, a heterogeneous azeotrope occurs in the liquid−liquid equili- brium (LLE) region where the liquid mixture is not completely miscible as shown in Figure S7. LLE occurred at low temperatures (e.g., below 220 K). The azeotropic VLE region crosses into the LLE region at normalized pressures, thus resulting in a heterogeneous azeotrope at $x_{HFC-125}$ = 0.550 and 217.0 K. Seven homogeneous and six heterogeneous azeotropes are predicted for the 21 binary mixtures as shown in Figure 2. Only a few LLE refrigerant systems have been experimentally confirmed (e.g., HFC-32/HC-290).[146−150]

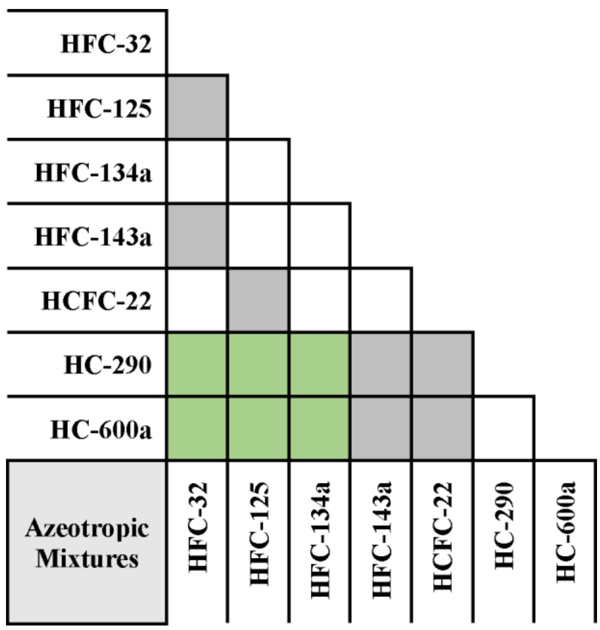

2.4. Ionic Liquid Solubility Regression.

The solubilities of the seven refrigerants in [C_4C_1im][PF_6] were regressed using the vdW1 mixing rule with the B−M method. The B−M method was required to improve the fit with experimental data (see Figures S9 in the SI). Since no literature data was available for HC-290 in [C_4C_1im][PF_6], the solubility was assumed to be the same as HC-290 in [C_2C_1im][Tf_2N].

Three experimental variables (*T*, *P*, and *x*) were regressed for each refrigerant in [C_4C_1im][PF_6]. In the case where LLE was observed, four experimental variables (*T*, *P*, $x_i^{(1)}$, and $x_i^{(2)}$) were included. The ML objective function was used with the same error values as the refrigerant binary regressions. The summary for all of the IL solubility data sets and regression results for parameters k_{ij} and l_{ij}, with the composition AAD, is shown in Table 4.[14,80,85,92,95,102,108] The results of the overall AAD in temperature and pressure can be found in the SI (see

Figure 2. Homogenous (gray) and heterogeneous (green) azeotropes for binary refrigerant mixtures at normalized pressures.

Table S7). For the two liquid compositions in the LLE data sets, AAD was estimated by considering both $x_i^{(1)}$ and $x_i^{(2)}$ as one variable, defined as "x_i" in Table 4.

Excluding the deviations in coordinates for the three LLE data sets, the average AAD in composition was 1.048 mol %,

Table 4. Refrigerant Solubility in $[C_4C_1im][PF_6]$ Regression Summary

(i)		N_{points}	N_{temp}	temperature range (K)	$k_{ij}^{(1)}$ ($\times 10^1$)	$k_{ij}^{(2)}$ ($\times 10^3$)	$l_{ij}^{(1)}$ ($\times 10^0$)	$l_{ij}^{(2)}$ ($\times 10^3$)	AAD x_i (%)	ref
HFC-32		31	4	283.15−348.15					1.23	80
		7[a]	1	298.15	0.900	−0.226	0.419	−1.117	1.67	14
HFC-125		36[a]	4	283.15−348.15					1.23	80
		7	1	298.15					*2.27*	14
	(LLE)	3	3	283.15−323.15	−2.963	1.243	0.233	−1.043	3.23	85
HFC-134a		32	4	283.15−348.15					1.13	80
	(LLE)	3	3	318.20−355.00	7.087	−2.219	2.576	−8.828	1.19	92
HFC-143a		36	4	285.15−348.15					1.10	80
	(LLE)	3	3	291.80−338.60	−1.860	1.261	−0.044	0.771	0.13	92
HCFC-22		47	4	283.15−348.15	−3.830	1.221	−0.860	2.554	0.78	95
HC-290[b]		16	4	304.00−352.00	−9.209	3.883	−1.904	6.422	0.03	102
HC-600a		30	6	288.15−313.15	9.944	−2.335	1.960	−6.565	0.01	108

[a]Data weight, w_d = 50. [b]Assumed to be the same solubility as in $[C_2C_1im][Tf_2N]$.

approximately 0.357 mol % larger than refrigerant binary systems. Some AADs were <1 mol % such as HCFC-22 (0.78 mol %), HC-290 (0.03 mol %), and HC-600a (0.01 mol %).

The average AAD for all deviations in temperature was 0.4 K, about the same as the refrigerant binary systems. The average AAD for all deviations in pressure was 3.326×10^{-4} MPa, about two orders of magnitude less than the refrigerant binary systems. The models compared with the experimental solubility data for the refrigerants in $[C_4C_1im][PF_6]$ are shown in Figure 3, and the data sets for HFC-32 and HFC-125 in $[C_4C_1im][PF_6]$ were weighted.

The hydrocarbons, HC-290 (see Figure 3f) and HC-600a (see Figure S8 in the SI), have very low solubility in $[C_4C_1im][PF_6]$ and large predicted LLE regions. LLE was also predicted for HFC-125, HFC-134a, and HFC-143a and has been confirmed experimentally. The solubilities for all seven refrigerants in $[C_4C_1im][PF_6]$ were compared at 298.15 K in Figure 4 and can be used to guide the process design for separating multicomponent mixtures. HC-290 is represented by a dashed line to remind the reader that the solubility is assumed, since there is no literature for the HC-290/ $[C_4C_1im][PF_6]$ system.

3. METHOD

Process designs developed for the separation of multi-component azeotropic refrigerant mixtures included the following unit operations: flash separation, conventional distillation, and extractive distillation. The distillation process requires the following variables to run a simulation: distillate rate (D), operating pressure (P), total number of theoretical stages (N_T), feed stage (N_F), reflux ratio (RR), feed temperature (T_F), and feed pressure (P_F). Extractive distillation also includes the following additional variables: solvent feed stage (N_S), solvent-to-feed (S/F) ratio, solvent feed temperature (T_S), and solvent feed pressure (P_S).

To limit the number of variables used in optimization, heuristics were first defined:

(i) A liquid-phase feed will result in a higher distillate purity compared to a vapor-phase feed, and the colder the refrigerant and solvent feeds, the higher the distillate purity. All feed temperatures were set at 293.15 K (ambient temperature), so no additional cooling of the streams was necessary. The feed pressure was set at 2.0 MPa and higher than the column operating pressure to ensure that the feed was in the liquid state.

(ii) The solvent feed stage (N_S) for an IL should enter at the top of the column ($N_S = 2$). Ionic liquids have essentially no measurable vapor pressure, and the feed stage is a function of the feed component's volatility.

(iii) The distillate rate (D) should equal the feed rate (F) of the light key component (or the sum of the light key components) to achieve complete component recovery at the desired purity.

Determining the light key (LK) or heavy key (HK) components of a multicomponent mixture can be difficult, especially where multiple azeotropes are present. With multiple azeotropes and large differences of component compositions, the LK cannot be optimized by order of boiling point, because some components can be completely distilled outside the order of boiling point. This work provides an original method to test if conventional distillation can be used for multicomponent mixtures in mass distilled versus distillate rate diagrams. The distillate rate (D) of a conventional distillation column (with specifications P = 1.0 MPa, N_T = 50, N_F/N_T = 0.5, and RR = 5) was varied from 0% to 100% of the feed to show the percentage of mass distilled for each component. Mass distilled versus distillate rate diagrams were prepared, and four examples are shown in Figure 5 (these diagrams are composition dependent). The dashed lines in these diagrams represent components that are distilled outside the order of boiling point; for example, in Figure 5d, HC-290 has a higher boiling point than HFC-32, but HC-290 was distilled out first. This confirms that these multicomponent azeotropic mixtures do not follow the order of boiling point when leaving the distillate.

The larger the vertical difference between the mass distilled lines, the greater the potential to separate LK and HK components. To achieve a complete separation, there needs to be a vertical break where the LK reaches 100% mass distilled, and the HK remains close to 0%. An example of this can be seen in Figure 5d where, at about 90% distillate rate, HFC-134a remained at 0% while the rest of the components reached 100%; in this case, for conventional distillation, HFC-32, HFC-125, HCFC-22, and HC-290 are defined as the LK components, and HFC-134a is the HK component.

If a difference between two sets of components is not conclusive, then extractive distillation should be considered. The LK and HK for extractive distillation are defined by comparing the solubilities of the components as previously shown in Figure 4. The solubilities of HFC-125, HFC-143a, HC-290, and HC-600a are much lower than components

https://doi.org/10.1021/acs.iecr.2c00937
Ind. Eng. Chem. Res. XXXX, XXX,

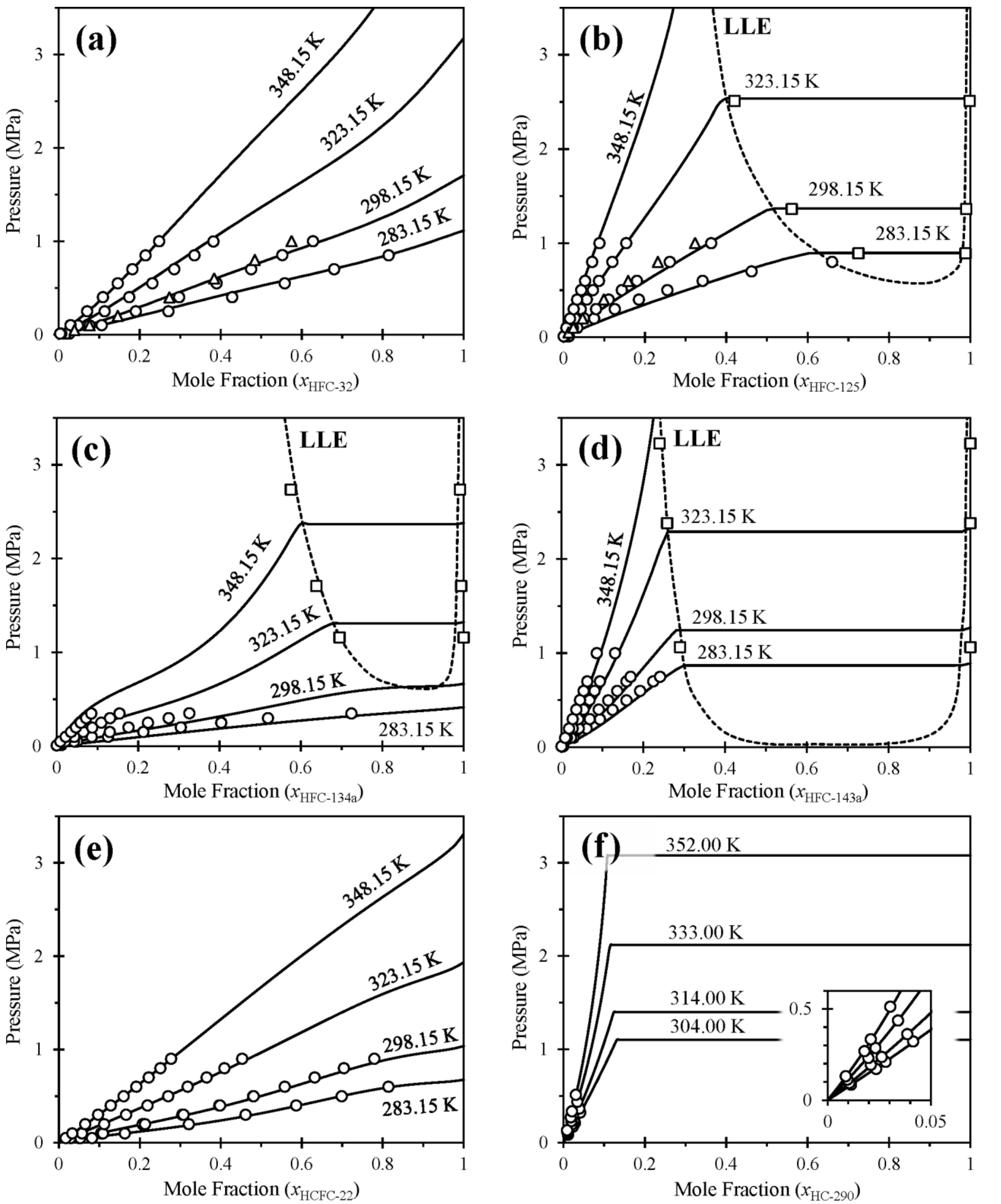

Figure 3. *PTx* data (○, Δ) for (a) HFC-32, (b) HFC-125, (c) HFC-134a, (d) HFC-143a, (e) HCFC-22, and (f) HC-290 with $[C_4C_1im][PF_6]$ and corresponding LLE data (□) for HFC-125, HFC-134a, and HFC-143a referenced in Table 4.

HFC-32, HFC-134a, and HCFC-22; therefore, in an extractive distillation process, HFC-125, HFC-143a, HC-290, and HC- 600a are expected to be in the distillate, identified as the LK components, and HFC-32, HFC-134a, and HCFC-22 are expected to remain in the entrainer with the bottom stream, identified as the HK components. We have observed that the narrower the range of solubility difference between the LK and HK (i.e., HFC-32 and HFC-125), the more *S*/*F* is required with increasing amounts of the HK.

The variables *P*, N_T, N_F, RR, and *S*/*F* were optimized to obtain the highest component purities within the following constraints. The minimum column pressure was set such that

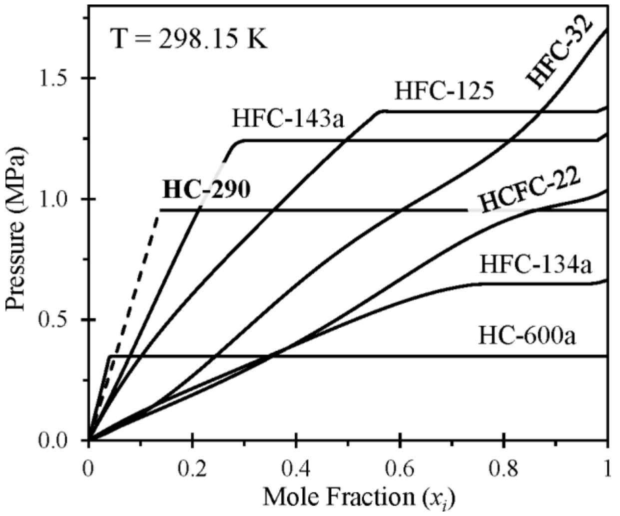

Figure 4. *PTx* regression lines for solubility of seven refrigerants in $[C_4C_1im][PF_6]$ at 298.15 K.

the condenser could operate with chilled water (i.e., T_{cond} > 293.15 K). A maximum reboiler temperature was specified (i.e., T_{reb} < 373.15 K) to avoid potential issues with IL decomposition. The reflux ratio (RR) was varied from 0.5 to 5, and the solvent-to-feed ratio (S/F) was varied from 0.5 to 10. Large values for the S/F ratio indicate an inefficient separation, and the IL was not selective to one of the feed components.

The first step in the optimization process was to determine D by defining the LK components. The LK components will then determine T_{cond} at different pressures. The N_F and RR were then varied to obtain the maximum distillate purity. If the desired purity (i.e., 99.5 wt %) could not be achieved using conventional distillation, the N_T was increased, and the optimization process was repeated. For systems that require conventional distillation with N_T > 50, extractive distillation was recommended for more efficient separation.

The optimization process for extractive distillation was similar. First, the optimum D, P, N_F, and RR were determined, and the S/F was increased until the desired purity of 99.5 wt % was achieved. If the desired purity could not be achieved, the N_T was increased, and the optimization process was repeated. Once the desired purity was achieved, the minimum reboiler duty (Q_{reb}) was determined by optimizing the P and S/F ratio at a specified product purity, where P was selected such that T_{cond} > 293.15 K and T_{reb} < 373.15 K. The initial conditions for the distillation processes were N_T = 20, N_F/N_T = 0.5, and RR = 2 and S/F = 5 for extractive distillation.

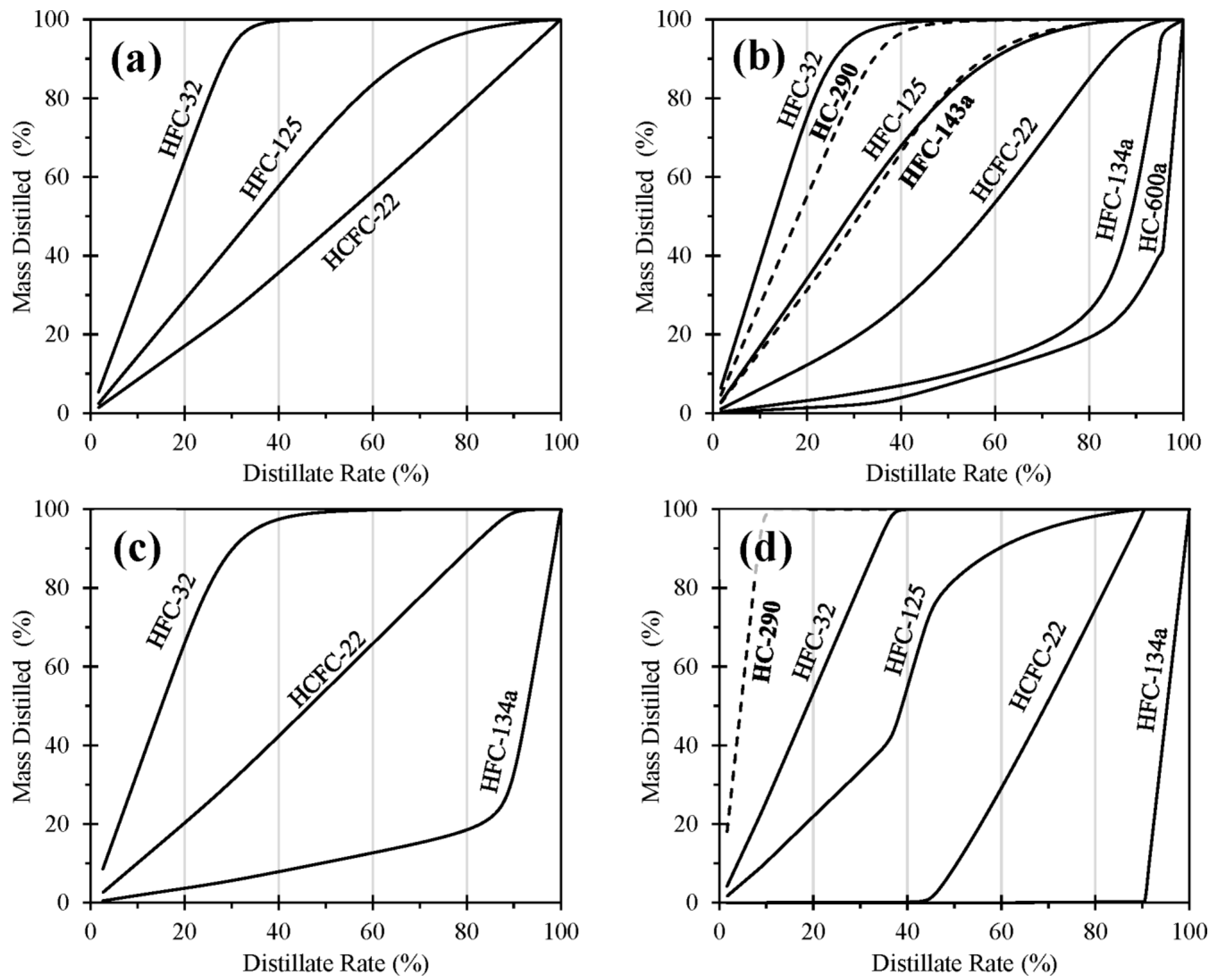

Figure 5. Mass distilled of each component vs the distillate rate for four different compositions.

https://doi.org/10.1021/acs.iecr.2c00937

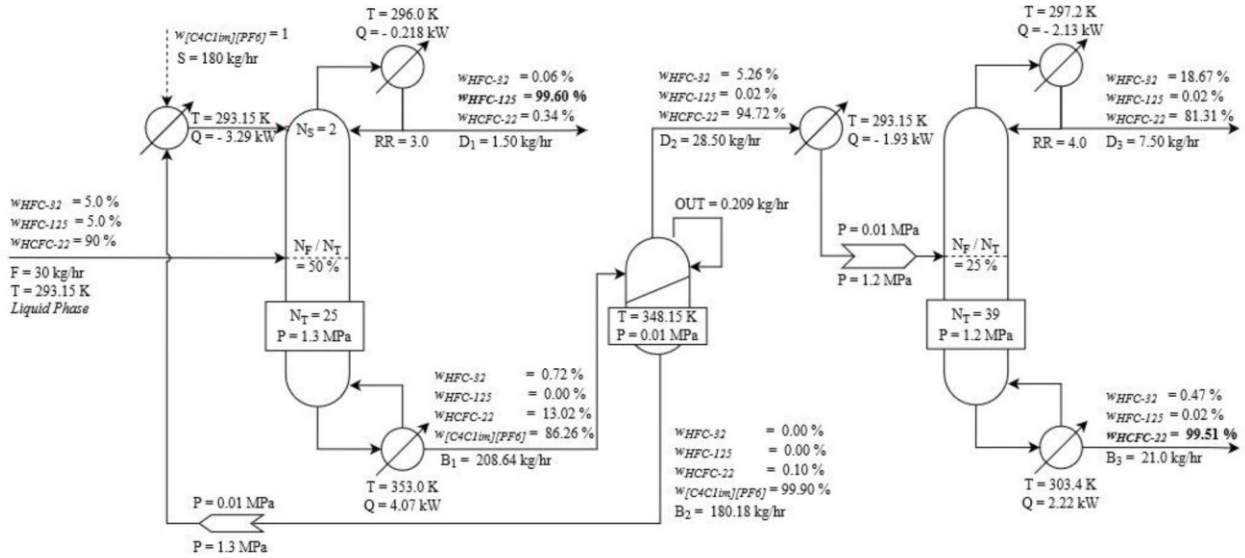

Figure 6. Process for recovering HCFC-22 containing 10 wt % R-410A with entrainer [C_4C_1im][PF_6].

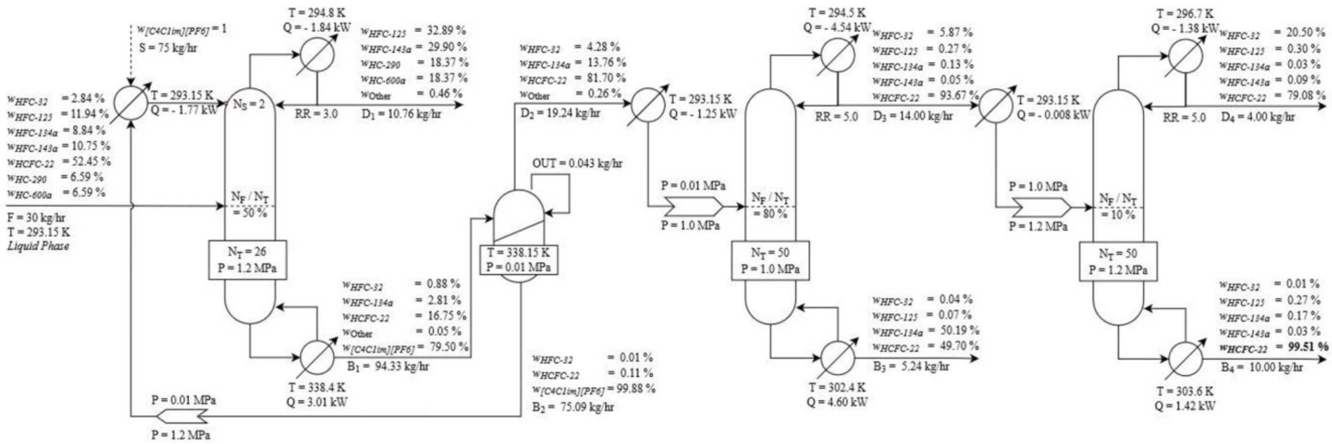

Figure 7. Process for recovering HCFC-22 from a seven-component mixture (hypothetical reclaimed refrigeration mixture) with entrainer [C_4C_1im][PF_6].

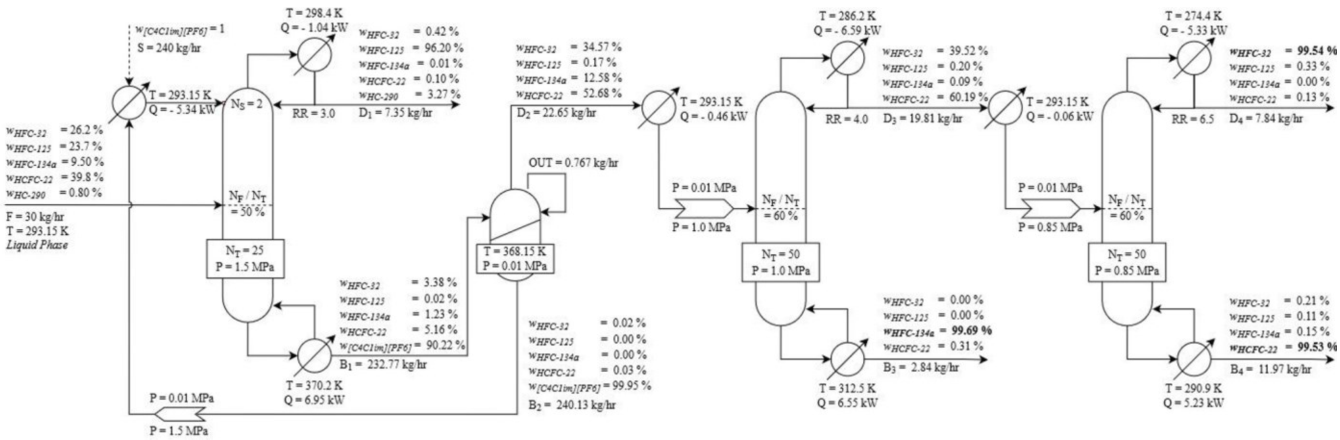

Figure 8. Process for separating a five-component mixture (hypothetical reclaimed HVAC mixture) with entrainer [C_4C_1im][PF_6].

A flash vessel was used for recovering and recycling the IL back to the extractive distillation column. The flash separation was a single stage equilibrium process and was only dependent on T and P. Since ILs are nonvolatile and have a very low vapor pressure (i.e., <1 × 10^{-5} Pa), only a single stage separation was required to remove the refrigerant. To ensure that 99.5 wt % of the refrigerant is recovered from the IL, the flash vessel was operated at T > 423.15 K or under vacuum conditions. To minimize the heat duty required for the flash vessel, the T was set to be similar to T_{reb}, and various pressures

https://doi.org/10.1021/acs.iecr.2c00937
Ind. Eng. Chem. Res. XXXX, XXX, XXX−XXX

from P = 0.01 to 0.1013 MPa were evaluated to maximize IL recovery. If higher IL recovery was required, the T of the flash was increased. Finally, a small amount of refrigerant (w_{ref} < 0.5 wt %) remaining in the recycled IL will decrease the viscosity of the fluid and reduce the pump power; however, this amount must be balanced with the purity required in the distillate from the extraction distillation column.

If the process does not achieve a satisfactory purity within the constraints of the system, additional methods for improving the distillate purity for conventional distillation include decreasing the column pressure and, for extractive distillation, include increasing the column pressure or S/F ratio. If neither of these approaches increase the distillate purity within the stated constraints, the D can be decreased, but this will reduce overall product recovery.

4. SIMULATION

ASPEN simulations were set up to model three common mixtures that are problematic for the refrigerant reclaim industry. The first simulation provides a process flow diagram (PFD) for separating HCFC-22 that is contaminated with 10 wt % R-410A, shown in Figure 6. The second simulation provides a PFD for recovering HCFC-22 from a multi- component mixture made up of HFC-32, HFC-125, HFC- 134a, HFC-143a, HC-290, and HC-600a shown in Figure 7. The third simulation provides a PFD for maximizing the recovery of all refrigerants in a 5-component mixture made up of HFC-32, HFC-125, HFC-134a, HCFC-22, and HC-290 shown in Figure 8.

The mass fractions (w_i), mass flow rates (F, S, B_n, and D_n), heat duties (Q), T, P, RR, feed locations (N_S and N_F), and the number of theoretical stages (N_T) are provided in Figures 6−8. In the vapor stream from the flash vessel, there is a trace amount of IL (defined as the "OUT" stream). The PR-EoS slightly overpredicts the vapor pressure for the IL, which accounts for this loss and was treated as an outlet that was recycled back to the column (similar to how a demister would be used if IL were entrained in the refrigerant vapor). The separations of the nonazeotropic binary systems were also investigated with conventional distillation to quantify the difficulty of separation.

4.1. Zeotropic Binary Separation.

8 of the 21 binary refrigerant mixtures were zeotropic (i.e., nonazeotropic) but can be classified as close-boiling systems (see Figure 2). A simulation was developed to quantify and rank the difficulty of separating a 50/50 wt % mixture by determining the minimum N_T to achieve a separation of 99.5 wt % for each component. The column and feed pressures were set to 1.0 and 2.0 MPa, respectively, and the feed temperature was set to 293.15 K. Initially, the RR was set to 1.0; however, this resulted in N_T > 100 for most of these cases, so a RR = 5 was selected and the results are shown in Table 5.

In some cases, such as binary mixtures containing HFC-125/ HFC-143a and HCFC-22/HFC-143a, a purity of 99.5 wt % with less than 100 stages was not possible unless the RR > 5. For example, with N_T = 100 and RR = 5.0, HFC-125/HFC- 143a achieved a maximum purity of about 59 wt % HFC-143a in the distillate, and HCFC-22/HFC-143a achieved a maximum purity of about 74 wt % of HFC-143a in the distillate. This was expected based on the small differences in the pure component boiling points.

The binary mixture HFC-134a/HFC-32 was the easiest to separate and only required 18 stages to reach a purity greater

Table 5. Nonazeotropic Binary Separations

heavy key	light key	ΔT_b (K)	N_T	N_F
HFC-134a	HFC-32	25.4	18	10
	HFC-125	22.2	32	16
	HFC-143a	21.3	36	17
	HCFC-22	14.5	89	61
HFC-143a	HFC-125	0.9	>100	
HCFC-22	HFC-32	10.9	47	30
	HFC-143a	6.8	>100	

than 99.5% for both components. Binary systems with HFC- 134a became increasingly harder to separate as the difference in the boiling temperature with the second component decreased, ΔT_b.

4.2. Simulation 1Recovering HCFC-22 from R-410A. Reclaimed HCFC-22 is still an important refrigerant used for servicing existing equipment and can often be contaminated with other refrigerants such as R-410A (50 wt % HFC-32 and 50 wt % HFC-125), which was developed as a replacement for HCFC-22. In our previous work, a process was developed to recover HFC-32 from a mixture of R-410A contaminated with 10 wt % HCFC-22. In this work, our goal is to maximize the recovery of HCFC-22 from a mixture contaminated with 10 wt % R-410A. In this ternary system, HFC-32/HFC-125 and HCFC-22/HFC-125 both form binary azeotropes; therefore, an extractive distillation process will be required for separating and purifying the HCFC-22.

To determine the LK and HK, a mass distilled versus distillate rate diagram of the feed composition was prepared and is shown in Figure 5a. A definitive separation where one or two components reach 100% mass distilled while the others remain close to 0% was not possible. For example, HFC-32 is the first component to be distilled but cannot be separated from HFC-125, and the distilled HFC-125 rate was also similar to HCFC-22; therefore, both HFC-32 and HFC-125 cannot be completely separated from HCFC-22. Extractive distillation must be used to separate this ternary mixture and the LK, and HK is defined by the solubility in the entrainer. HFC-32 and HCFC-22 have a much larger solubility than HFC-125 (see Figure 4) in [C_4C_1im][PF_6]; therefore, HFC-125 will be the LK, and HFC-32 and HCFC-22 will be entrained with the IL as the HKs.

A feed composition of 90 wt % HCFC-22, 5 wt % HFC-32, and 5 wt % HFC-125 was fed into the first column at F = 30 kg/h and T = 293.15 K. The distillate rate was set to D = 1.5 kg/h so the column could be optimized for maximizing the separation of HFC-125 (e.g., 99.5 wt % purity and recovery). The first column operated at P = 1.3 MPa so that T_{cond} > 293.15 K. The P, RR, and S/F ratio have little effect on the optimal N_F (±1). A sensitivity analysis was conducted on N_F to maximize HFC-125 purity in the distillate, and the optimal feed stage was found to be 0.5 N_F/N_T. The reflux ratio was varied from RR = 0.0 to 5.0. The purity of HFC-125 in the distillate reached a maximum at about RR = 3.0. Increasing RR > 3 provided diminishing returns on purity, so the reflux ratio was set at RR = 3.0. The solvent feed rate was increased until the HFC-125 distillate achieved >99.5 wt % purity. If the HFC-125 purity did not achieve 99.5 wt % in the distillate, then the N_T would have to be increased. If N_T was increased, then the solvent feed rate should also be optimized. The minimum N_T to reach the target purity was 25 with S/F = 6 and RR = 3.

https://doi.org/10.1021/acs.iecr.2c00937

The heat duty Q_{reb} was minimized by conducting a sensitivity analysis of the P and S/F ratio while maintaining a purity of >99.5 wt % HFC-125 in the distillate. The P was varied from 1.3 MPa (i.e., T_{cond} > 293.15 K) to where T_{reb} < 373.15 K. The S/F ratio was varied from 0.5 to 10 in increments of 0.5. A pressure of P = 1.3 MPa and S/F = 6 resulted in the minimum reboiler duty of Q_{reb} = 4.07 kW with T_{reb} = 354.2 K.

The bottom stream from the extractive distillation column that contains IL with HCFC-22 and HFC-32 was fed to a flash tank operating at 348.15 K and 0.01 MPa to separate the refrigerants from [C_4C_1im][PF_6]. The IL was recycled back to the extractive distillation column, and the vapor stream from the flash tank contained 94.7 wt % HCFC-22 and 5.3 wt % HFC-125. The vapor was cooled to 293.15 K and fed to a second conventional distillation column. HFC-32 and HCFC- 22 are zeotropic, but close-boiling components (ΔT_b = 10.9 °C). The separation was possible with conventional distillation but difficult due to the similar boiling points and narrow VLE region. Extractive distillation could also be used to increase the efficiency in separating HFC-32 and HCFC-22, but a new IL entrainer would be required since both refrigerants have a high solubility in [C_4C_1im][PF_6].

The conventional distillation was set at the maximum stages of N_T = 50 (i.e., constraint). The optimal RR was 4.0 with minimal improvement in separation at higher reflux ratios. Even with the maximum number of stages (N_T = 50), this system could not achieve a purity of 99.5 wt % for HFC-32 and HCFC-22. In this case, there are two options to increase purity for conventional distillation: (1) decrease the column pressure or (2) reduce the distillate rate. To maintain T_{cond} > 293.2 K (i.e., constraint) and avoid low-temperature distillation, the distillate rate was increased incrementally by 0.5 kg/h to increase the purity of the HCFC-22 in the bottoms stream.

The maximum amount of HCFC-22 that could be recovered with a purity of 99.51 wt % HCFC-22 and 0.47 wt % HFC-32 was 21 kg/h. The overall HCFC-22 recovery was 78 wt %. The distillate from the conventional distillation column (D_3 = 7.50 kg/h) was considered a waste stream with 81.31 wt % HCFC- 22 and 18.67 wt % HFC-32. The addition of a second IL extraction could be used to recover additional HCFC-22 but was not considered in this analysis. Overall, this process was able to recover 100 wt % of the HFC-125 (1.5 kg/h) and 78 wt % of the HCFC-22 (21 kg/h) with purities exceeding 99.5 wt %.

4.3. Simulation 2Recovering HCFC-22 from a Multicomponent Refrigerant Separation. A process simulation was developed to recover HCFC-22 from a hypothetical reclaimed multicomponent mixture with a composition based on market trends for a refrigeration application (see Figure 7 and Table 1). To separate the seven components into the LK and HK, a mass distilled versus distillate rate diagram of the feed composition was prepared similar to the previous simulation and is shown in Figure 5b. The components HCFC-22 and HFC-134a show a vertical trend at higher distillate rates, but the area below those two curves shows that only about 20% of HFC-134a and HC-600 will end up in the distillate and cannot be completely separated from the rest of the components. A definitive separation of the components for defining an LK and HK was possible as shown in Figure 5b; therefore, an extractive distillation simulation was developed. HFC-32, HCFC-22, and HFC-134a have a much higher solubility in [C_4C_1im][PF_6] than HFC-125, HFC-143a,

https://doi.org/10.1021/acs.iecr.2c00937

HC-290, and HC-600a (see Figure 4). The lower solubility components (HFC-125, HFC-143a, HC-290, and HC-600a) were specified as the LK components, and the distillate rate was set to the sum of these feed flow rates, D = 10.76 kg/h.

The feed entered the first column at 30 kg/h and T = 293.15 K. The pressure was set to P = 1.2 MPa so that T_{cond} > 293.15 K (i.e., constraint). The optimal feed stage was set at $0.5N_F/N_T$ similar to the previous simulation, and the optimal RR was again about 3.0. As stated previously, a higher RR would result in a higher purity separation, but RR > 3.0 did not significantly increase the distillate purity and reduced overall recovery of products in the distillate. The recovery of the LK components was 99.5% with N_T = 26 and S/F = 2.5. The minimum Q_{reb} was 3.01 kW with T_{reb} = 338.4 K. The LK components form an azeotropic mixture that can be further separated using extractive distillation but would require an alternate solvent with a higher selectivity for the components than $[C_4C_1im]$- $[PF_6]$.

The HKs are separated from the IL in a flash vessel operated at T = 338.2 K and P = 0.01 MPa. The largest impurities in the LK and HK are HFC-125 and HFC-32, respectively. The HCFC-22 was flashed out of the IL and fed into a conventional distillation column where HCFC-22 was separated from HFC-32 and HFC-134a. Binary mixtures between these components (e.g., HFC-32, HFC-125, and HFC-134a) are close-boiling, but are not azeotropic (see Figure 3), and all three components have high solubility in $[C_4C_1im][PF_6]$ (see Figure 4), so extractive distillation could not be used.

To determine the LK and HK for HFC-32, HFC-134a, and HCFC-22, a mass distilled versus distillate rate diagram of the feed composition was developed and is shown in Figure 5c. At about a 90% distillate rate, 100 wt % HFC-32 and HCFC-22 can be distilled while about 20 wt % HFC-134a remained in the distillate. The 20 wt % HFC-134a can be minimized; thus, HFC-32 and HCFC-22 are the LK, and HFC-134a is the HK. The distillate rate was set to the sum of HFC-32 and HCFC- 22, D = 16.59 kg/h.

The convention distillation was set with maximum conditions of N_T = 50 and RR = 5.0 (i.e., constraints), and the optimized N_F for this system could not achieve 99.5 wt % HCFC-22. A pressure of 1.0 MPa was selected to avoid low distillation temperatures. A distillate containing 93.67 wt % HCFC-22 at a flow rate of D_3 = 14 kg/h was produced. The bottoms stream (B_3 = 5.24 kg/h) contained 50.19 wt % HFC- 134a and 49.70 wt % HCFC-22 and was disregarded as a waste stream. The distillate (D_3 = 14 kg/h) was fed into a second distillation column to separate the zeotropic mixture HFC-32 and HCFC-22.

The second distillation column could also not reach a purity of 99.5 wt % in the distillate at N_T = 50 and RR = 5. The distillate rate was decreased and P set to 1.2 MPa, so T_{cond} > 293.15 K. The bottoms of the second conventional distillation column resulted in a product of 99.51 wt % HCFC-22 with a total flow rate of B_3 = 10 kg/h (63.6 wt % recovery). The distillate stream that contained 20.50 wt % HFC-32 and 79.08 wt % HCFC-22 with a flow rate of D_4 = 4.00 kg/h was regarded as a waste stream. Overall, this seven-component refrigerant mixture was composed of HFC-32, HFC-125, HFC-134a, HFC-143a, HCFC-22, HC-290, and HC-600a.

The HC-600a was a challenge to separate, and only 10 kg of HCFC-22 was able to be recovered while 20 kg of the remaining components would need to be disposed of or utilized as a fluorinated feedstock for producing other

https://doi.org/10.1021/acs.iecr.2c00937

products. This example highlights the challenges in separating multicomponent azeotropic refrigerant mixtures.

4.4. Simulation 3 Complete Separation of a Multicomponent Refrigerant Separation. For the final simulation, a process, shown in Figure 8, was developed to separate a mixture containing HFC-32, HFC-125, HFC-134a, HCFC-22, and HC-290 into individual components with a purity >99.5 wt %. The hypothetical mixture composition was based on a reclaimed refrigerant mixture using market trends for the HVAC industry (see Table 1). To separate the five components into the LK and HK, a mass distilled versus distillate rate diagram of the feed composition was developed and is shown in Figure 5d.

HFC-134a remained at 0% while the rest of the components reached 100% at around a 90% distillate rate; therefore, in this case, conventional distillation could be used to separate HFC-134a from the other components. A conventional distillation column was optimized with HFC-134a in the bottoms and achieved a purity of 99.58 wt % with column specifications of $N_T = 50$, RR = 5, and $P = 1.0$ MPa ($T_{cond} = 285.0$ K). Since purity could not be achieved within the defined constraints of T_{cond}, extractive distillation was used.

HFC-125 and HC-290 have low solubility in $[C_4C_1im][PF_6]$ and were distilled out as the LK, while HFC-32, HFC-134a, and HCFC-22 were entrained and exit as the HK with the IL (see Figure 4). The distillate rate was set to the sum of the LK, $D = 7.35$ kg/h.

The feed entered the first column (i.e., extractive distillation column) at 30 kg/h and $T = 293.15$ K. The pressure was set to 1.5 MPa, and the optimal feed stage was at $0.5N_F/N_T$; similarly to the previous processes, RR plateaued around 3.0 and was set to 3.0. This resulted in a separation requiring a minimum of $N_T = 25$ to reach >99.5 wt % of the LK components, HFC-125 and HC-290, and $S/F = 8$ resulted in a minimum $Q_{reb} = 6.95$ kW and $T_{reb} = 370.2$ K. This process required much more solvent than the previous two simulations, possibly in relation to having more HFC-125 in the distillate. HFC-125 and HC-290 form an azeotropic mixture that could then be further separated with extractive distillation but would require an alternate solvent with a higher selectivity of the components than $[C_4C_1im][PF_6]$. The bottoms of the extractive distillation column was then fed into a flash vessel that was set to 368.2 K and allowed for solvent recovery at 0.01 MPa.

The HK components, HFC-32, HFC-134a, and HCFC-22, are near-boiling but are not azeotropic. As in the previous simulation, HFC-32 and HCFC-22 were the LK, and HFC-134a was the HK in the first column; HFC-32 was the LK, and HCFC-22 was the HK in the second column.

The second process column (i.e., first conventional distillation column) was set with maximum conditions of $N_T = 50$ and RR = 5.0, and at the optimized N_F, this system could not reach complete separation. The RR = 4.0 produced similar purities, so the RR was decreased to 4.0. Since the goal of this simulation was to achieve a complete separation of all components, the full distillate rate heuristic remained, and P was decreased. A new column pressure ($P = 1.0$ MPa) was tested so that $T_{cond} > 283.2$ K. The condensing and reboiler temperatures were $T_{cond} = 286.2$ K and $T_{reb} = 312.5$ K, respectively. The bottoms stream resulted in 99.69 wt % HFC-134a, and the distillate was fed into the third process column (i.e., second conventional distillation column), which operated at similar conditions but required a lower operating pressure ($P = 0.85$ MPa) to maintain $T_{cond} > 273.2$ K. The reboiler since HFC-125/HCFC-22 and HFC-32/

https://doi.org/10.1021/acs.iecr.2c00937

temperature (T_{reb} = 290.9 K) was below ambient temperatures, so this was considered a low-temperature operation. Achieving >99.5 wt % purity by separating HCFC-22 and HFC-32 with N_T = 50 and P = 0.85 MPa could only be achieved by increasing the RR < 5.0. At an RR = 6.5, the distillate and bottoms stream resulted in 99.54 wt % HFC-32 and 99.54 wt % HCFC-22.

As shown in Figure 8, this five-component mixture separation is challenging. Three of the five components (HFC-134a, HFC-32, and HCFC-22) could be separated with a purity >99.5 wt %. The HFC-125 + HC-290 separation remains a challenge, and a purity of only 96.2 wt % HFC-125 was achieved in the distillate of the extractive distillation. Future research will investigate new IL entrainers for efficiently separating hydrocarbons from HFCs

5. CONCLUSIONS

Multicomponent refrigerant mixtures that form azeotropes can be separated using extractive distillation with IL entrainers. The purified refrigerants can be recycled and used for making new refrigerant mixtures (e.g., HFC/HFO blends) and repurposed as fluorinated feedstocks for future low-global- warming products. Many refrigerants such as HFCs, HCFCs, and HCs form azeotropes that cannot be separated using conventional distillation and will require advanced techniques such as extractive distillation. Ionic liquids provide the opportunity to tune the solubility of refrigerants to maximize separation efficiency. Extractive distillation with ILs is a developing field with only two papers published on experimental designs and less than 40 articles published on process simulations.

Limited data for the solubility of refrigerants in ILs was available, and future research should focus on measuring and modeling the phase behavior of these systems (e.g., VLE for HCFC-22/HFC-125 and HCFC-22/HC-600a). Currently, there are only three ILs ([C_4C_1im][PF_6], [C_2C_1im][Tf_2N], and [C_6C_1im][Tf_2N]) with solubility data available for all seven refrigerants (HCFC-22, HFC-32, HFC-125, HFC-134a, HFC-143a, HC-290, and HC-600a) studied in this work, and the IL [C_4C_1im][PF_6] was selected as the entrainer for this work. Refrigerants HFC-32, HFC-134a, and HCFC-22 had higher solubility compared to HFC-125, HFC-143a, HC-290, and HC-600 in [C_4C_1im][PF_6].

Before simulations can be conducted, binary equilibrium data, such as VLE and LLE, need to be regressed to define the binary parameters for each system. Binary refrigerant data was regressed using the PR-EoS with the vdW1 mixing rule to define k_{ij} and B−M correction to define l_{ij} for highly nonideal systems. Six heterogeneous and seven homogeneous azeo- tropes were predicted at ambient pressures, and eight binary systems were zeotropic.

A set of heuristics and constraints were defined and simulations conducted for conventional and extractive distillation. Mass distilled versus distillate rate plots were created to assist in defining the LK and HK components for each unit operation. Variables P, RR, N_T/N_F, and S/F were optimized to minimize Q_{reb} and N_T to achieve >99.5 wt % refrigerant purities. Equilibrium models were used to complete three simulations.

A process flow diagram was developed to recover HCFC-22 from a ternary refrigerant mixture contaminated with R-410A. None of the components could be separated using conven- tional distillation

HFC-125 formed azeotropes, so extractive distillation was used. The components with the higher solubility (e.g., HFC-32 and HCFC-22) were entrained with the IL and removed from the IL using a flash process. The vapor stream from the flash vessel was fed into a conventional distillation column that produced a bottoms stream (21 kg/h) containing 99.51 wt % HCFC-22. The overall recover of HCFC-22 was 78 wt %.

A second process was developed to recover HCFC-22 from a seven-component refrigerant mixture. None of the components could be separated with conventional distillation. Extractive distillation was used to separate the higher-solubility components (e.g., HFC-32, HFC-134a, and HCFC-22) in the IL entrainer. The vapor stream from the flash vessel was fed into a conventional distillation column where HFC-134a was separated from HCFC-22. A second conventional distillation column was required to purify the HCFC-22 in the bottoms stream to 99.51 wt % with a flow rate of 10 kg/h. The overall recovery of HCFC-22 was 63.6 wt %. The separation of the seven refrigerants was challenging, and overall, 20 kg/h of mixed refrigerant remained that would need to be further processed, destroyed, or utilized as a fluorinated feedstock to produce other products.

The third simulation provided a process design that can separate a five-component refrigerant mixture. The mixture contained HCFC-22, HFC-32, HFC-125, HFC-134a, and HC-290. The HFC-134a could be separated initially as the HK using a conventional distillation, but extractive distillation was required in order to separate the HFC-125. The distillate of the extractive distillation column contained 96.20 wt % HFC- 125 and 3.27 wt % HC-290. This azeotropic mixture could not be further purified. A new IL entrainer with higher selectivity for one of the components will be required to achieve a purity of 99.5 wt % HFC-125 in the extractive distillation process. Separation of HC-290 from many of the HFCs was problematic due to the number of azeotropes that this hydrocarbon forms. The components with a higher solubility in the IL (e.g., HFC-32, HFC-134a, and HCFC-22) were absorbed in the entrainer. To achieve a complete separation of HFC-32, HFC-134a, and HCFC-22, the *P* and RR constraints had to be expanded. The vapor stream from the flash vessel was fed into a conventional distillation column where the HFC-134a (HK) of the first column resulted in 99.69 wt % HFC-134a. The distillate was then fed into a second distillation column that had to operate at lower than ambient temper- atures. The distillate and bottom streams of the second column resulted in 99.54 wt % HFC-32 and 99.53 wt % HCFC-22. Overall, more than 75 wt % of the multicomponent mixture could be separated into the original components (HCFC-22, HFC-32, and HFC-134a) with purities greater than 99.5 wt %. Future work should include finding new IL entrainers for separating binary refrigerant systems such as HFC-32/HCFC- 22, HFC-125/HFC-143a, and HFC-125/HC-290. In addition, rate-based models should be developed to assist with sizing future conventional and extractive distillation columns. Addi- tional properties will be required for rate-based models such as density, viscosity, surface tension, and liquid heat capacity for refrigerants and ILs, and this provides another area for future research.

ASSOCIATED CONTENT

*Supporting Information

The Supporting Information is available free of charge at https://pubs.acs.org/doi/10.1021/acs.iecr.2c00937.

Table of global refrigerants distribution; nomenclature for anion and cation names in ionic liquids; summary of all simulation papers of extractive distillation with ionic liquids; pseudoproperties for [C_4C_1im][PF_6]; ideal heat capacity as a function of temperature for [C_4C_1im]- [PF_6]; error analysis formulas; regression summaries including all AAD for each experimental coordinate; figures of regressed *TPxy* data for refrigerant binary systems; example figure predicting a heterogeneous azeotrope for the HFC-125/HC-290 system; regressed *PTx* data for HC-600a with [C_4C_1im][PF_6]; and a figure showing the comparison of IL solubility with and without the B−M mixing rule (PDF)

AUTHOR INFORMATION

Corresponding Author

Mark B. Shiflett − *Institute for Sustainable Engineering, University of Kansas, Lawrence, Kansas 66045, United States; Department of Chemical and Petroleum Engineering, University of Kansas, Lawrence, Kansas 66045, United States;* orcid.org/0000-0002-8934-6192; Email: Mark.B.Shiflett@ku.edu

Authors

Ethan A. Finberg − *Institute for Sustainable Engineering, University of Kansas, Lawrence, Kansas 66045, United States; Department of Chemical and Petroleum Engineering, University of Kansas, Lawrence, Kansas 66045, United States;* orcid.org/0000-0002-4702-016X

Tessie L. May − *Institute for Sustainable Engineering, University of Kansas, Lawrence, Kansas 66045, United States; Department of Chemical and Petroleum Engineering, University of Kansas, Lawrence, Kansas 66045, United States;* orcid.org/0000-0002-3000-9765

Complete contact information is available at: https://pubs.acs.org/10.1021/acs.iecr.2c00937

Notes

The authors declare no competing financial interest.

REFERENCES

(1) Farman, J. C.; Gardiner, B. G.; Shanklin, J. D. Large losses of total ozone in Antarctica reveal seasonal ClOx/NOx interaction. *Nature* 1985, *315* (1), 207−210.

(2) Wuebbles, D. J. Chlorocarbon emission scenarios: potential impact on stratospheric ozone. *Journal of Geophysical Research* 1983, *88* (C2), 1433−1443.

(3) Houghton, J. T.; Jenkins, G. J.; Ephraums, J. J. *Climate Change: The IPCC Scientific Assessment*; Cambridge University Press: Cam- bridge, UK, 1990. https://www.ipcc.ch/report/ar1/wg1/ (accessed 2022-03-18).

(4) *High-GWP Refrigerants|California Air Resources Board*. https://ww2.arb.ca.gov/resources/documents/high-gwp-refrigerants (accessed 2021-09-09).

(5) United States Environmental Protection Agency. *Inventory of U.S. Greenhouse Gas Emissions and Sinks: 1990−2019 Data Highlights*. https://nepis.epa.gov/Exe/ZyPURL.cgi?Dockey=P10127UD.txt (ac- cessed 2022-03-18).

(6) *United Nations Framework Convention on Climate Change: What is the Kyoto Protocol?* https://unfccc.int/kyoto_protocol (accessed 2022-03-18).

(7) *EU legislation to control F-gases*. https://ec.europa.eu/clima/ policies/f-gas/legislation_en (accessed 2021-06-14).

(8) *Montreal Protocol on Substances that Deplete the Ozone Layer*. https://www.environment.gov.au/protection/ozone/montreal-protocol (accessed 2021-06-14).

(9) *Recent International Developments under the Montreal Protocol*. https://www.epa.gov/ozone-layer-protection/recent-international- developments-under-montreal-protocol (accessed 2021-06-14).

(10) *AIM Act*. https://www.epa.gov/climate-hfcs-reduction/aim-act (accessed 2021-06-14).

(11) Booten, C.; Nicholson, S.; Mann, M.; Abdelaziz, O. *Refrigerants: Market Trends and Supply Chain Assessment*; Technical Report NREL/TP-5500-0207, Contract DE-AC36-08GO28308; Clean Energy Manufacturing Analysis Center: Golden, CO, 2020.

(12) Calm, J. M.; Didion, D. A. Trade-offs in refrigerant selections: past, present, and future. *International Journal of Refrigeration* 1998, *21* (4), 308−321.

(13) Wang, H.; Tung, H. S. *Process for the Manufacture of Fluorinated Olefins*. EP17170975A1, 2018.

(14) Morais, A. R. C.; Harders, A. N.; Baca, K. R.; Olsen, G. M.; Befort, B. J.; Dowling, A. W.; Maginn, E. J.; Shiflett, M. B. Phase Equilibria, Diffusivities, and Equation of State Modeling of HFC-32 and HFC-125 in Imidazolium-Based Ionic Liquids for the Separation of R-410A. *Ind. Eng. Chem. Res.* 2020, *59* (40), 18222−18235.

(15) Baca, K. R.; Broom, D.; Roper, M.; Benham, M.; Shiflett, M. B. First measurements for the simultaneous sorption of Difluoromethane and Pentafluoroethane mixtures in Ionic Liquids using the new Hiden XEMIS gravimetric microbalance with the Integral Mass Balance method. *Ind. Eng. Chem. Res.* 2022, in press. DOI: 10.1021/ acs.iecr.2c00497

(16) Yancey, A. D.; Terian, S. J.; Shaw, B. J.; Bish, T. M.; Corbin, D. R.; Shiflett, M. B. A Review of Fluorocarbon Sorption on Porous Materials. *Microporous Mesoporous Mater.* 2022, *331*, 111654.

(17) Harders, A. N.; Sturd, E. R.; Vallier, J. E.; Corbin, D. R.; Whitney, W.; Junk, C. P.; Shiflett, M. B. Selective Separation of HFC- 32 from R-410A using poly(dimethylsiloxane) and a copolymer of perfluoro(butenyl vinyl ether) and perfluoro(2,2-dimethyl-1,3-diox- ole). *J. Membr. Sci.* 2022, *652*, 120467.

(18) Drout, W. M. Extractive Distillation Process. U.S. Patent US2610141, 1952.

(19) Doherty, M. F.; Malone, M. F. *Conceptual Design of Distillation Systems*, 1st ed.; McGraw-Hill Companies, Inc.: New York, 2001; p 568.

(20) Doherty, M. F.; Knapp, J. P. Distillation, Azeotropic, and Extractive. In *Kirk-Othmer Encyclopedia of Chemical Technology*; John Wiley & Sons, Inc., 2004; Vol. *8*, pp 358−398.

(21) Lei, Z.; Li, C.; Chen, B. Extractive Distillation: A Review. *Separation and Purification Reviews* 2003, *32* (2), 121−213.

(22) Lei, Z.; Dai, C.; Zhu, J.; Chen, B. Extractive Distillation with Ionic Liquids: A Review. *AIChE J.* 2014, *60* (9), 3312−3329.

(23) Meindersma, G. W.; Quijada-Maldonado, E.; Jongmans, M. T. G.; Hernandez, J. P. G.; Schuur, B.; de Haan, A. B. Extractive Distillation with Ionic Liquids: Pilot Plant Experiments and Conceptual Process Design. *Ionic Liquids for Better Separation Processes* 2015, *1* (1), 11−38.

(24) Werner, S.; Haumann, M.; Wasserscheid, P. Ionic Liquids in Chemical Engineering. *Annu. Rev. Chem. Biomol. Eng.* 2010, *1* (1), 203−230.

(25) Song, D.; Seibert, A. F.; Rochelle, G. T. Mass Transfer Parameters for Packings: Effect of Viscosity. *Ind. Eng. Chem. Res.* 2018, *57* (2), 718−729.

(26) Mellein, B. R.; Scurto, A. M.; Shiflett, M. B. Gas solubility in ionic liquids. *Current Opinion in Green and Sustainable Chemistry* 2021, *28*, 100425.

(27) Shiflett, M. B.; Maginn, E. J. The Solubility of Gases in Ionic Liquids. *AIChE J.* 2017, *63* (11), 4722−4737.

(28) Lei, Z.; Dai, C.; Chen, B. Gas Solubility in Ionic Liquids. *Chem. Rev.* 2014, *114* (2), 1289−1326.

(29) Pereiro, A. B.; Araújo, J. M. M.; Esperança, J. M. S. S.; Marrucho, I. M.; Rebelo, L. P. N. Ionic liquids in separations of

azeotropic systems − A review. *J. Chem. Thermodyn.* 2012, *46* (1), 2−28.
(30) Arlt, W.; Seiler, M.; Jork, C.; Schneider, T. *Ionic Liquids as Selective Additives for Separation of Close-Boiling or Azeotropic Mixtures*. U.S. Patent US2004/0133058A1, 2004.
(31) Beste, Y. A.; Shoenmakers, H.; Arlt, W.; Seiler, M.; Jork, C. *Recycling of ionic liquids produced in extractive distillation*. U.S. Patent US2006/0272934A1, 2006.
(32) Massonne, K. *Ionic Liquids at BASF SE*. http://www.wet.kuleuven.be/english/summerschools/ionicliquids/lectures/massonne.pdf (accessed 2020-03-03).
(33) Meindersma, G. W.; Quijada-Maldonado, E.; Aelmans, T. A. M.; Hernandez, J. P. G.; de Haan, A. B. Ionic Liquids in Extractive Distillation of Ethanol/Water: From Laboratory to Pilot Plant. In *Ionic Liquids: Science and Applications*; Visser, A. E., Bridges, N. J., Rogers, R. D., Eds.; American Chemical Society: Washington, DC, 2012; Vol. *1117*, pp 239−257.
(34) Song, Z.; Li, X.; Chao, H.; Mo, F.; Zhou, T.; Cheng, H.; Chen, L.; Qi, Z. Computer-aided ionic liquid design for alkane/cycloalkane extractive distillation process. *Green Energy & Environment* 2019, *4* (2), 154−165.
(35) Wu, L.; Wu, L.; Liu, Y.; Guo, X.; Hu, Y.; Cao, R.; Pu, X.; Wang, X. Conceptual design for the extractive distillation of cyclopentane and neohexane using a mixture of N,N-dimethyl formamide and ionic liquid as the solvent. *Chem. Eng. Res. Des.* 2018, *129* (1), 197−208.
(36) Ayuso, M.; Cañada-Barcala, A.; Larriba, M.; Navarro, P.; Delgado-Mellado, N.; García, J.; Rodríguez, F. Enhanced separation of benzene and cyclohexane by homogeneous extractive distillation using ionic liquids as entrainers. *Sep. Purif. Technol.* 2020, *240*, 116583.
(37) Li, W.; Xu, B.; Lei, Z.; Dai, C. Separation of benzene and cyclohexane by extractive distillation intensified with ionic liquid. *Chemical Engineering and Processing: Process Intensification* 2018, *126* (1), 81−89.
(38) Navarro, P.; Ayuso, M.; Palma, A. M.; Larriba, M.; Delgado-Mellado, N.; Garcia, J.; Rodriguez, F.; Coutinho, J. A. P.; Carvalho, P. J. Toluene/n-Heptane Separation by Extractive Distillation with Tricyanomethanide-Based Ionic Liquids: Experimental and CPA EoS Modeling. *Ind. Eng. Chem. Res.* 2018, *57* (42), 14242−14253.
(39) Quijada-Maldonado, E.; Meindersma, G. W.; de Haan, A. B. Pilot plant study on the extractive distillation of toluene−methylcyclohexane mixtures using NMP and the ionic liquid [hmim][TCB] as solvents. *Sep. Purif. Technol.* 2016, *166* (1), 196−204.
(40) Díaz, I.; Palomar, J.; Rodríguez, M.; de Riva, J.; Ferro, V.; González, E. J. Ionic liquids as entrainers for the separation of aromatic−aliphatic hydrocarbon mixtures by extractive distillation. *Chem. Eng. Res. Des.* 2016, *115* (1), 382−393.
(41) Navarro, P.; de Dios-García, I.; Larriba, M.; Delgado-Mellado, N.; Ayuso, M.; Moreno, D.; Palomar, J.; García, J.; Rodríguez, F. Dearomatization of pyrolysis gasoline by extractive distillation with 1- ethyl-3-methylimidazolium tricyanomethanide. *Fuel Process. Technol.* 2019, *195*, 106156.
(42) Jongmans, M. T. G.; Hermens, E.; Raijmakers, M.; Maassen, J. I. W.; Schuur, B.; de Haan, A. B. Conceptual process design of extractive distillation processes for ethylbenzene/styrene separation. *Chem. Eng. Res. Des.* 2012, *90* (12), 2086−2100.
(43) Meindersma, G. W.; Quijada-Maldonado, E.; Jongmans, M. T. G.; Hernandez, J. P. G.; Schuur, B.; de Haan, A. B. Extractive Distillation with Ionic Liquids: Pilot Plant Experiments and Conceptual Process Design. In *Ionic Liquids for Better Separation Processes*; Springer: Berlin, Heidelberg, 2016; pp 11−38.
(44) Jiang, Y.; Taheri, M.; Yu, G.; Zhu, J.; Lei, Z. Experiments, Modeling, and Simulation of CO_2 Dehydration by Ionic Liquid, Triethylene Glycol, and Their Binary Mixtures. *Ind. Eng. Chem. Res.* 2019, *58* (34), 15588−15597.
(45) Meindersma, G. W.; Quijada-Maldonado, E.; Aelmans, T. A. M.; Hernandez, J. P. G.; de Haan, A. B. Ionic Liquids in Extractive Distillation of Ethanol/Water: From Laboratory to Pilot Plant. *Ionic Liquids: Science and Applications* 2012, *1117*, 239−257.

(46) Quijada-Maldonado, E.; Aelmans, T. A. M.; Meindersma, G. W.; de Haan, A. B. Pilot plant validation of a rate-based extractive distillation model for water−ethanol separation with the ionic liquid [emim][DCA] as solvent. *Chemical Engineering Journal* 2013, *223* (1), 287−297.

(47) Quijada-Maldonado, E.; Meindersma, G. W.; de Haan, A. B. Ionic liquid effects on mass transfer efficiency in extractive distillationof water−ethanol mixtures. *Comput. Chem. Eng.* 2014, *71* (1), 210−219.

(48) Quijada-Maldonado, E.; Meindersma, G. W.; de Haan, A. B. Mass Transfer in Extractive Distillation when Using Ionic Liquids as Solvents. In *Heat and Mass Transfer—Advances in Modelling and Experimental Study for Industrial Applications*; Ren, Y., Ed.; InTechOpen, 2018; pp 107−123.

(49) Zhu, Z.; Ri, Y.; Li, M.; Jia, H.; Wang, Y.; Wang, Y. Extractive distillation for ethanol dehydration using imidazolium-based ionic liquids as solvents. *Chemical Engineering and Processing: Process Intensification* 2016, *109* (1), 190−198.

(50) Ramírez-Corona, N.; Ek, N.; Jiménez-Gutiérrez, A. A method for the design of distillation systems aided by ionic liquids. *Chemical Engineering and Processing: Process Intensification* 2015, *87* (1), 1−8.

(51) Figueroa, J. E. J.; Rodrigues, M. I.; Maciel, M. R. W. Sequential strategy of experimental design I: Optimization of extractive distillation process of ethanol−water using [bmim][N(CN)2] as entrainer. *Chemical Engineering and Processing: Process Intensification* 2015, *93* (1), 56−60.

(52) Álvarez, V. H.; Alijó, P.; Serrão, D.; Filho, R. M.; Aznar, M.; Mattedi, S. Production of Anhydrous Ethanol by Extractive Distillation of Diluted Alcoholic Solutions with Ionic Liquids. *Comput.-Aided Chem. Eng.* 2009, *27* (1), 1137−1142.

(53) Figueroa, J. E. J.; Lunelli, B. H.; Filho, R. M.; Maciel, M. R. W. Improvements on Anhydrous Ethanol Production by Extractive Distillation using Ionic Liquid as Solvent. *Procedia Engineering* 2012, *42* (1), 1016−1026.

(54) Seiler, M.; Jork, C.; Kavarnou, A.; Arlt, W.; Hirsch, R. Separation of Azeotropic Mixtures Using Hyperbranched Polymers or Ionic Liquids. *AIChE J.* 2004, *50* (10), 2439−2454.

(55) Aniya, V.; De, D.; Satyavathi, B. Comprehensive Approach toward Dehydration of tert-Butyl Alcohol by Extractive Distillation: Entrainer Selection, Thermodynamic Modeling and Process Opti- mization. *Ind. Eng. Chem. Res.* 2016, *55* (25), 6982−6995.

(56) Li, J.; Li, T.; Peng, C.; Liu, H. Extractive Distillation with Ionic Liquid Entrainers for the Separation of Acetonitrile and Water. *Ind. Eng. Chem. Res.* 2019, *58* (14), 5602−5612.

(57) Chen, H. H.; Chen, M. K.; Chen, B. C.; Chien, I. L. Critical Assessment of Using an Ionic Liquid as Entrainer via Extractive Distillation. *Ind. Eng. Chem. Res.* 2017, *56* (27), 7768−7782.

(58) Ma, S.; Shang, X.; Zhu, M.; Li, J.; Sun, L. Design, optimization and control of extractive distillation for the separation of isopropanol- water using ionic liquids. *Sep. Purif. Technol.* 2019, *209* (1), 833−850.

(59) Zhu, Z.; Geng, X.; He, W.; Chen, C.; Wang, Y.; Gao, J. Computer-Aided Screening of Ionic Liquids As Entrainers for Separating Methyl Acetate and Methanol via Extractive Distillation. *Ind. Eng. Chem. Res.* 2018, *57* (29), 9656−9664.

(60) Zhu, Z.; Ri, Y.; Jia, H.; Li, X.; Wang, Y.; Wang, Y. Process evaluation on the separation of ethyl acetate and ethanol using extractive distillation with ionic liquid. *Sep. Purif. Technol.* 2017, *181* (1), 44−52.

(61) Cao, Z.; Wu, X.; Wei, X. Ionic liquid screening for desulfurization of coke oven gas based on COSMO-SAC model and process simulation. *Chem. Eng. Res. Des.* 2021, *176* (1), 146−161.

(62) Zhu, Z.; Hu, J.; Geng, X.; Qin, B.; Ma, K.; Wang, Y.; Gao, J. Process design of carbon dioxide and ethane separation using ionic liquid by extractive distillation. *J. Chem. Technol. Biotechnol.* 2018, *93* (3), 887−896.

(63) Shiflett, M. B.; Shiflett, A. D.; Yokozeki, A. Separation of tetrafluoroethylene and carbon dioxide using ionic liquids. *Sep. Purif. Technol.* 2011, *79* (3), 357−364.

(64) Shiflett, M. B.; Yokozeki, A. Separation of difluoromethane and pentafluoroethane by extractive distillation using ionic liquid. *Chemistry Today* 2006, *24* (2), 28−30.
(65) Asensio-Delgado, S.; Pardo, F.; Zarca, G.; Urtiaga, A. Absorption separation of fluorinated refrigerant gases with ionic liquids: Equilibrium, mass transport, and process design. *Sep. Purif. Technol.* 2021, *276*, 119363.
(66) Finberg, E. A.; Shiflett, M. B. Process Designs for Separating R- 410A, R-404A, and R-407C Using Extractive Distillation and Ionic Liquid Entrainers. *Ind. Eng. Chem. Res.* 2021, *60* (44), 16054−16067.
(67) Lei, Z.; Zhang, J.; Li, Q.; Chen, B. UNIFAC Model for Ionic Liquids. *Ind. Eng. Chem. Res.* 2009, *48* (5), 2697−2704.
(68) Dong, Y.; Guo, Y.; Zhu, R.; Zhang, J.; Lei, Z. UNIFAC Model for Ionic Liquids. 2. Revision and Extension. *Ind. Eng. Chem. Res.* 2020, *59* (21), 10172−10184.
(69) Lin, S.-T.; Sandler, S. I. A Priori Phase Equilibrium Prediction from a Segment Contribution Solvation Model. *Ind. Eng. Chem. Res.* 2002, *41* (5), 899−913.
(70) Renon, H.; Prausnitz, J. M. Local compositions in thermodynamic excess functions for liquid mixtures. *AIChE J.* 1968, *14* (1), 135−144.
(71) Kontogeorgis, G. M.; Voutsas, E. C.; Yakoumis, I. V.; Tassios, D. P. An equation of state for associating fluids. *Ind. Eng. Chem. Res.* 1996, *35* (11), 4310−4318.
(72) Chapman, W. G.; Gubbins, K. E.; Jackson, G.; Radosz, M. SAFT: Equation-of-state solution model for associating fluids. *Fluid Phase Equilib.* 1989, *52* (1), 31−38.
(73) Sosa, J. E.; Ribeiro, R. P. P. L.; Castro, P. J.; Mota, J. P. B.; Araujo, J. M. M.; Pereiro, A. B. Absorption of Fluorinated Greenhouse Gases Using Fluorinated Ionic Liquids. *Ind. Eng. Chem. Res.* 2019, *58* (45), 20769−20778.
(74) Asensio-Delgado, S.; Pardo, F.; Zarca, G.; Urtiaga, A. Vapor−Liquid Equilibria and Diffusion Coefficients of Difluoromethane, 1,1,1,2-Tetrafluoroethane, and 2,3,3,3-Tetrafluoropropene in Low-Viscosity Ionic Liquids. *Journal of Chemical & Engineering Data* 2020, *65* (9), 4242−4251.
(75) Shiflett, M. B.; Harmer, M. A.; Junk, C. P.; Yokozeki, A. Solubility and Diffusivity of Difluoromethane in Room-Temperature Ionic Liquids. *Journal of Chemical & Engineering Data* 2006, *51* (2), 483−495.
(76) Shiflett, M. B.; Yokozeki, A. *Absorption cycle utilizing ionic liquid as working fluid*. U.S. Patent US2006/0197053A1, 2006.
(77) Baca, K. R.; Olsen, G. M.; Valenciano, L. M.; Bennett, M. G.; Haggard, D. M.; Befort, B. J.; Garciadiego, A.; Dowling, A. W.; Maginn, E. J.; Shiflett, M. B. Phase Equilibria and Diffusivities of HFC-32 and HFC-125 in Ionic Liquids for the Separation of R-410A. *ACS Sustainable Chem. Eng.* 2022, *10* (2), 816−830.
(78) Dong, L.; Zheng, D.; Sun, G.; Wu, X. Vapor−Liquid Equilibrium Measurements of Difluoromethane + [Emim]OTf, Difluoromethane + [Bmim]OTf, Difluoroethane + [Emim]OTf, and Difluoroethane + [Bmim]OTf Systems. *Journal of Chemical & Engineering Data* 2011, *56* (9), 3663−3668.
(79) Asensio-Delgado, S.; Pardo, F.; Zarca, G.; Urtiaga, A. Enhanced absorption separation of hydrofluorocarbon/hydrofluoroolefin refrig- erant blends using ionic liquids. *Sep. Purif. Technol.* 2020, *249* (1), 117136.
(80) Shiflett, M. B.; Yokozeki, A. Solubility and diffusivity of hydrofluorocarbons in room-temperature ionic liquids. *AIChE J.* 2006, *52* (3), 1205−1219.
(81) Liu, X.; He, M.; Lv, N.; Qi, X.; Su, C. Vapor−Liquid Equilibrium of Three Hydrofluorocarbons with [HMIM][Tf_2N]. *Journal of Chemical & Engineering Data* 2015, *60* (5), 1354−1361.
(82) Liu, X.; Lv, N.; Su, C.; He, M. Solubilities of R32, R245fa, R227ea and R236fa in a phosphonium-based ionic liquid. *J. Mol. Liq.* 2016, *218* (1), 525−530.
(83) Shiflett, M. B.; Yokozeki, A. Binary Vapor−Liquid and Vapor− Liquid−Liquid Equilibria of Hydrofluorocarbons (HFC-125 and HFC-143a) and Hydrofluoroethers (HFE-125 and HFE-143a) with

Ionic Liquid [emim][Tf2N]. *Journal of Chemical & Engineering Data* 2008, *53* (2), 492−497.

(84) Asensio-Delgado, S.; Viar, M.; Pardo, F.; Zarca, G.; Urtiaga, A. Gas solubility and diffusivity of hydrofluorocarbons and hydro- fluoroolefins in cyanide-based ionic liquids for the separation of refrigerant mixtures. *Fluid Phase Equilib.* 2021, *549*, 113210.

(85) Shiflett, M. B.; Yokozeki, A. Vapor−Liquid−Liquid Equilibria of Pentafluoroethane and Ionic Liquid [bmim][PF6] Mixtures Studied with the Volumetric Method. *J. Phys. Chem. B* 2006, *110* (29), 14436−14443.

(86) Liu, X.; Qi, X.; Lv, N.; He, M. Gaseous absorption of fluorinated ethanes by ionic liquids. *Fluid Phase Equilib.* 2015, *405* (1), 1−6.

(87) Shiflett, M. B.; Harmer, M. A.; Junk, C. P.; Yokozeki, A. Solubility and diffusivity of 1,1,1,2-tetrafluoroethane in room-temperature ionic liquids. *Fluid Phase Equilib.* 2006, *242* (2), 220−232.

(88) Ren, W.; Scurto, A. M. Phase equilibria of imidazolium ionic liquids and the refrigerant gas, 1,1,1,2-tetrafluoroethane (R-134a). *Fluid Phase Equilib.* 2009, *286* (1), 1−7.

(89) Ren, W.; Scurto, A. M.; Shiflett, M. B.; Yokozeki, A. Phase Behavior and Equilibria of Ionic Liquids and Refrigerants: 1-Ethyl-3- methyl-imidazolium Bis(trifluoromethylsulfonyl)imide ([EMIm]- [Tf_2N]) and R-134a. *Gas-Expanded Liquids and Near-Critical Media* 2009, *1006* (1), 112−128.

(90) Lepre, L. F.; Andre, D.; Denis-Quanquin, S.; Gautier, A.; Pádua, A. A. H.; Gomes, M. C. Ionic Liquids Can Enable the Recycling of Fluorinated Greenhouse Gases. *ACS Sustainable Chem. Eng.* 2019, *7* (19), 16900−16906.

(91) Shiflett, M. B.; Yokozeki, A. Solubility Differences of Halocarbon Isomers in Ionic Liquid [emim][Tf_2N]. *Journal of Chemical & Engineering Data* 2007, *52* (5), 2007−2015.

(92) Shiflett, M. B.; Yokozeki, A. Vapor−Liquid−Liquid Equilibria of Hydrofluorocarbons + 1-Butyl-3-methylimidazolium Hexafluoro- phosphate. *Journal of Chemical & Engineering Data* 2006, *51* (5), 1931−1939.

(93) Ahosseini, A.; Ren, W.; Weatherley, L. R.; Scurto, A. M. Viscosity and self-diffusivity of ionic liquids with compressed hydrofluorocarbons: 1-Hexyl-3-methyl-imidazolium bis-(trifluoromethylsulfonyl)amide and 1,1,1,2-tetrafluoroethane. *Fluid Phase Equilib.* 2017, *437* (1), 34−42.

(94) Liu, X.; He, M.; Lv, N.; Qi, X.; Su, C. Solubilities of R-161 and R-143a in 1-Hexyl-3-methylimidazolium bis(trifluoromethylsulfonyl)- imide. *Fluid Phase Equilib.* 2015, *388* (1), 37−42.

(95) Minnick, D. L.; Shiflett, M. B. Solubility and Diffusivity of Chlorodifluoromethane in Imidazolium Ionic Liquids: [emim][Tf_2N], [bmim][BF_4], [bmim][PF_6], and [emim][TFES]. *Ind. Eng. Chem. Res.* 2019, *58* (25), 11072−11081.

(96) Sun, Y.; Di, G.; Wang, J.; Hu, Y.; Wang, X.; He, M. Gaseous solubility and thermodynamic performance of absorption system using R1234yf/IL working pairs. *Applied Thermal Engineering* 2020, *172* (1), 115161.

(97) Sun, Y.; Zhang, Y.; Wang, X.; Prausnitz, J. M.; Jin, L. Gaseous absorption of 2,3,3,3-tetrafluoroprop-1-ene in three imidazolium- based ionic liquids. *Fluid Phase Equilib.* 2017, *450* (1), 65−74.

(98) Esaki, T.; Kobayashi, N. Experimental absorption solubility and rate of hydrofluoroolefin refrigerant in ionic liquids for absorption chiller cycles. *Chem. Eng. Res. Des.* 2021, *171* (1), 340−348.

(99) Zhang, Y.; Yin, J.; Wang, X. Vapor-liquid equilibrium of 2,3,3,3- tetrafluoroprop-1-ene with 1-butyl-3-methylimidazolium hexafluoro- phosphate, 1-hexyl-3-methyl imidazolium hexafluorophosphate, and 1-octyl-3-methylimidazolium hexafluorophosphate. *J. Mol. Liq.* 2018, *260* (1), 203−208.

(100) Liu, X.; Ye, Z.; Bai, L.; He, M. Performance comparison of two absorption-compression hybrid refrigeration systems using R1234yf/ ionic liquid as working pair. *Energy Conversion and Management* 2019, *181* (1), 319−330.

(101) Liu, X.; Bai, L.; Liu, S.; He, M. Vapor−Liquid Equilibrium of R1234yf/[HMIM][Tf_2N] and R1234ze(E)/[HMIM][Tf_2N] Work-

Q

ing Pairs for the Absorption Refrigeration Cycle. *Journal of Chemical & Engineering Data* 2016, *61* (11), 3952−3957.

(102) Liu, X.; Afzal, W.; Prausnitz, J. M. Solubilities of Small Hydrocarbons in Tetrabutylphosphonium Bis(2,4,4-trimethylpentyl) Phosphinate and in 1-Ethyl-3-methylimidazolium Bis- (trifluoromethylsulfonyl)imide. *Ind. Eng. Chem. Res.* 2013, *52* (42), 14975−14978.

(103) Lee, B.-C.; Outcalt, S. L. Solubilities of Gases in the Ionic Liquid 1-n-Butyl-3-methylimidazolium Bis(trifluoromethylsulfonyl)-imide. *Journal of Chemical & Engineering Data* 2006, *51* (3), 892−897.

(104) Kim, Y. S.; Jang, J. H.; Lim, B. D.; Kang, J. W.; Lee, C. S. Solubility of mixed gases containing carbon dioxide in ionic liquids: Measurements and predictions. *Fluid Phase Equilib.* 2007, *256* (2), 70−74.

(105) Sun, Y.; Wang, J.; Wei, Q.; Wang, X. Solubility for Propane and Isobutane in [P66614]Cl from 278.15 to 348.15 K. *Journal of Chemical & Engineering Data* 2021, *66* (3), 1273−1279.

(106) Liu, X.; Afzal, W.; Yu, G.; He, M.; Prausnitz, J. M. High Solubilities of Small Hydrocarbons in Trihexyl Tetradecylphospho- nium Bis(2,4,4-trimethylpentyl) Phosphinate. *J. Phys. Chem. B* 2013, *117* (36), 10534−10539.

(107) Pison, L.; Bernales, V.; Fuentealba, P.; Padua, A. A. H.; Gomesa, M. F. C. Isobutane as a probe of the structure of 1-alkyl-3- methylimidazolium bis(trifluoromethylsulfonyl)imide ionic liquids. *J. Chem. Thermodyn.* 2015, *89* (1), 98−103.

(108) Zhang, Y.; Zhang, T.; Gan, P.; Li, H.; Zhang, M.; Jin, K.; Tang, S. Solubility of Isobutane in Ionic Liquids [BMIm][PF_6], [BMIm][BF_4], and [BMIm][Tf_2N]. *Journal of Chemical & Engineering Data* 2015, *60* (6), 1706−1714.

(109) Liu, X.; He, M.; Lv, N.; Qi, X.; Su, C. Solubilities of isobutane and cyclopropane in ionic liquids. *J. Chem. Thermodyn.* 2015, *88* (1), 30−35.

(110) He, M.; Peng, S.; Liu, X.; Pan, P.; He, Y. Diffusion coefficients and Henry's constants of hydrofluorocarbons in [HMIM][Tf_2N], [HMIM][TfO], and [HMIM][BF_4]. *J. Chem. Thermodyn.* 2017, *112* (1), 43−51.

(111) Camper, D.; Becker, C.; Koval, C.; Noble, R. Low Pressure Hydrocarbon Solubility in Room Temperature Ionic Liquids Containing Imidazolium Rings Interpreted Using Regular Solution Theory. *Ind. Eng. Chem. Res.* 2005, *44* (6), 1928−1933.

(112) Fallanza, M.; Ortiz, A.; Gorri, D.; Ortiz, I. Propylene and Propane Solubility in Imidazolium, Pyridinium, and Tetralkylammo- nium Based Ionic Liquids Containing a Silver Salt. *Journal of Chemical & Engineering Data* 2013, *58* (8), 2147−2153.

(113) Kazakov, A. F.; Magee, J. W.; Chirico, R. D.; Diky, V.; Kroenlein, K. G.; Muzny, C. D.; Frenkel, M. D. *Ionic Liquids Database*−*ILThermo (v2.0)*. https://ilthermo.boulder.nist.gov (ac- cessed 2021-09-12).

(114) Peng, D.-Y.; Robinson, D. B. A New Two-Constant Equation of State. *Industrial & Engineering Chemistry Fundementals* 1976, *15* (1), 59−64.

(115) Valderrama, J. O.; Rojas, R. E. Critical Properties of Ionic Liquids. Revisited. *Ind. Eng. Chem. Res.* 2009, *48* (14), 6890−6900.

(116) Valderrama, J. O.; Robles, P. A. Critical Properties, Normal Boiling Temperatures, and Acentric Factors of Fifty Ionic Liquids. *Ind. Eng. Chem. Res.* 2007, *46* (4), 1338−1344.

(117) Ge, R.; Hardacre, C.; Jacquemin, J.; Nancarrow, P.; Rooney, D. W. Heat Capacities of Ionic Liquids as a Function of Temperature at 0.1 MPa. Measurement and Prediction. *Journal of Chemical & Engineering Data* 2008, *53* (9), 2148−2153.

(118) Mathias, P. M.; Klotz, H. C.; Prausnitz, J. M. Equation-of-State mixing rules for multicomponent mixtures: the problem of invariance. *Fluid Phase Equilib.* 1991, *67* (1), 31−44.

(119) Cam, L. L. Maximum Likelihood: An Introduction. *Interna- tional Statistical Review* 1990, *58* (2), 153−171.

(120) Hou, S.-X.; Duan, Y.-Y.; Wang, X.-D. Vapor−Liquid Equilibria Predictions for New Refrigerant Mixtures Based on Group Contribution Theory. *Ind. Eng. Chem. Res.* 2007, *46* (26), 9274−9284.

https://doi.org/10.1021/acs.iecr.2c00937

(121) *The Chemours Company*. https://www.chemours.com/en (accessed 2022-03-18).

(122) Kang, Y. W.; Chung, K. Y. Vapor−Liquid Equilibria for the Systems Difluoromethane + Chlorodifluoromethane, Difluorome- thane + Dichlorodifluoromethane, and Difluoromethane + Chloro- methane at 10.0 °C. *Chemical* & *Engineering Data* 1996, *41* (3), 443−445.

(123) Arita, K.; Tomizawa, T.; Nagakawa, Y.; Yoshida, Y. Vapour liquid equilibrium of the non-azeotropic refrigerant mixture formed by chlorofluoromethane and 1,1,1,2-tetrafluoroethane. *Fluid Phase Equilib.* 1991, *63* (1−2), 151−156.

(124) Nishiumi, H.; Komatsu, M.; Yokoyama, T.; Kohmatsu, S. Two- and three-phase equilibria and critical locus for the system of HCFC22-HFC134a. *Fluid Phase Equilib.* 1993, *83* (1), 109−117.

(125) Weber, L. A.; Silva, A. M. Design of a high-pressure ebulliometer, with vapor-liquid equilibrium results for the systems CHF_2Cl + CF_3CH_3 and CF_3CH_2F + CH_2F_2. *Int. J. Thermophys.* 1996, *17* (4), 873−888.

(126) Nagahama, K.; Hoshino, D.; Hirata, M. Vapor-Liquid Equilibria of Binary and Ternary Systems Containing $CHClF_2$, C_2ClF_5, and C_3H_8 at 273.15 K. In *World Congress III of Chemical Engineering*; Keio Plaza Hotel: Tokyo, Japan, 1986; Vol. *2*, pp 100− 103.

(127) Han, X.; Chen, G.; Cui, X.; Wang, Q. Vapor−Liquid Equilibrium Data for the Binary Mixture Difluoroethane (HFC-32) + Pentafluoroethane (HFC-125) of an Alternative Refrigerant. *Journal of Chemical* & *Engineering Data* 2007, *52* (6), 2112−2116.

(128) Cui, X.; Chen, G.; Li, C.; Han, X. Vapor−liquid equilibrium of difluoromethane + 1,1,1,2-tetrafluoroethane systems over a temper- ature range from 258.15 to 343.15 K. *Fluid Phase Equilib.* 2006, *249* (1−2), 97−103.

(129) Kim, C. N.; Park, Y. M. Vapor−Liquid Equilibria for the Difluoromethane (HFC-32) + 1,1,1-Trifluoroethane (HFC-143a) System. *Journal of Chemical* & *Engineering Data* 2000, *45* (1), 34−37.

(130) Kim, J. H.; Kim, M. S.; Kim, Y. Vapor−liquid equilibria for pentafluoroethane + propane and difluoromethane + propane systems over a temperature range from 253.15 to 323.15 K. *Fluid Phase Equilib.* 2003, *211* (2), 273−287.

(131) Akasaka, R.; Higashi, Y.; Tanaka, K.; Kayukawa, Y.; Fujii, K. Vapor−liquid equilibrium measurements and correlations for the binary mixture of difluoromethane + isobutane and the ternary mixture of propane + isobutane + difluoromethane. *Fluid Phase Equilib.* 2007, *261* (1−2), 286−291.

(132) Lim, J. S.; Park, J.-Y.; Lee, B.-G.; Lee, Y.-W.; Kim, J.-D. Reply to Comments by Stanislaw K. Malanowski and Roman Stryjek on J. Chem. Eng. Data 1999, 44, 1226−1230. *Journal of Chemical* & *Engineering Data* 2000, *45* (6), 1219−1221.

(133) Kim, C. N.; Park, Y. M. Vapor−Liquid Equilibrium of HFC-32/134a And HFC-125/134a Systems. *Int. J. Thermophys.* 1999, *20* (1), 519−530.

(134) Kato, R.; Nishiumi, H. Vapor−liquid equilibria and critical loci of binary and ternary systems composed of CH_2F_2, C_2HF_5 and $C_2H_2F_4$. *Fluid Phase Equilib.* 2006, *249* (1−2), 140−146.

(135) Higashi, Y. Vapor−Liquid Equilibrium, Coexistence Curve, and Critical Locus for Pentafluoroethane + 1,1,1-Trifluoroethane (R125/R143a). *Journal of Chemical* & *Engineering Data* 1999, *44* (2), 333−337.

(136) Lee, B. G.; Park, J. Y.; Lim, J. S.; Lee, Y. W.; Lee, C. H. Vapor−Liquid Equilibria for Isobutane + Pentafluoroethane (HFC- 125) at 293.15 to 313.15 K and + 1,1,1,2,3,3,3-Heptafluoropropane (HFC-227ea) at 303.15 to 323.15 K. *Journal of Chemical* & *Engineering Data* 2000, *45* (5), 760−763.

(137) Kim, C. N.; Lee, E.-H.; Park, Y. M.; Yoo, J.; Kim, K.-H.; Lim, J. S.; Lee, B. G. Vapor−Liquid Equilibria for the 1,1,1-Trifluoroethane (HFC-143a)+1,1,1,2-Tetrafluoroethane (HFC-134a) System. *Int. J. Thermophys.* 2000, *21* (1), 871−881.

(138) Lim, J. S.; Park, J. Y.; Kang, J. W.; Lee, B. G. Measurement of vapor−liquid equilibria for the binary systems of propane + 1,1,1,2-

tetrafluoroethane and 1,1,1-trifluoroethane + propane at various temperatures. *Fluid Phase Equilib.* 2006, *243* (1−2), 57−63.

(139) Bobbo, S.; Stryjek, R.; Elvassore, N.; Bertucco, A. A recirculation apparatus for vapor−liquid equilibrium measurements of refrigerants. Binary mixtures of R600a, R134a and R236fa. *Fluid Phase Equilib.* 1998, *150−151* (1), 343−352.

(140) Lim, J. S.; Park, J.-Y.; Lee, B.-G. High pressure vapor-liquid equilibria of binary system 1,1,1-trifluoroethane (HFC-143a)+pro- pane (HC-290). *Korean Journal of Chemical Engineering* 2005, *22* (1), 932−937.

(141) Im, J.; Lee, G.; Shin, M. S.; Lee, J.; Kim, H. Vapor−liquid equilibria of the 1,1,1-trifluoroethane (HFC-143a) + propane (HC- 290) system. *Fluid Phase Equilib.* 2006, *248* (1), 19−23.

(142) Lim, J. S.; Park, J.-Y.; Lee, B.-G.; Kim, J.-D. Phase Equilibria of Chlorofluorocarbon Alternative Refrigerant Mixtures. Binary Systems of Trifluoromethane + Isobutane at 283.15 and 293.15 K and 1,1,1-Trifluoroethane + Isobutane at 323.15 and 333.15 K. *Journal of Chemical & Engineering Data* 2000, *45* (5), 734−737.

(143) Bobbo, S.; Fedele, L.; Camporese, R.; Stryjek, R. VLE measurements and modeling for the strongly positive azeotropic R32+propane system. *Fluid Phase Equilib.* 2002, *199* (2), 175−183.

(144) Bobbo, S.; Fedele, L.; Camporese, R.; Stryjek, R. Hydrogen- bonding of HFCs with dimethyl ether: evaluation by isothermal VLE measurements. *Fluid Phase Equilib.* 2002, *199* (2), 153−160.

(145) Lim, J. S.; Park, J. Y.; Lee, K.-S.; Kim, J.-D.; Lee, B. G. Measurement of Vapor−Liquid Equilibria for the Binary Mixture of Pentafluoroethane (HFC-125) + Propane (R-290). *Journal of Chemical & Engineering Data* 2004, *49* (4), 750−755.

(146) Bobbo, S.; Fedele, L.; Camporese, R.; Stryjek, R. VLLE measurements and their correlation for the R32 + R600 system. *Fluid Phase Equilib.* 2003, *210* (1), 45−56.

(147) Fedele, L.; Bobbo, S.; Camporese, R.; Stryjek, R. VLLE measurements and correlation for the pentafluoroethane (R125) + n- butane (R600) system. *Fluid Phase Equilib.* 2004, *222* (1), 283−289.

(148) Dong, X.; Zhao, Y.; Gong, M.; Hao, G.; Wu, J. (Vapour + liquid + liquid) equilibrium measurements and correlation for the {1,1,1,2-tetrafluoroethane (R134a) + n-butane (R600)} system. *J. Chem. Thermodyn.* 2015, *84* (1), 87−92.

(149) Zhao, Y.; Gong, M.; Dong, X.; Hao, G.; Wu, J. (Vapor + liquid + liquid) equilibrium measurements and correlation for {1,1,2,2- tetrafluoroethane (R134) + isobutane (R600a)} system. *J. Chem. Thermodyn.* 2014, *78* (1), 182−188.

(150) Bobbo, S.; Fedele, L.; Camporese, R.; Scattolini, M.; Stryjek, R. Mutual solubility and VLLE correlation for the R32 + R290 system. *Fluid Phase Equilib.* 2003, *212* (2), 245−255.

https://doi.org/10.1021/acs.iecr.2c00937